Modeling of communication channels for analog and digital broadcast reception in cars

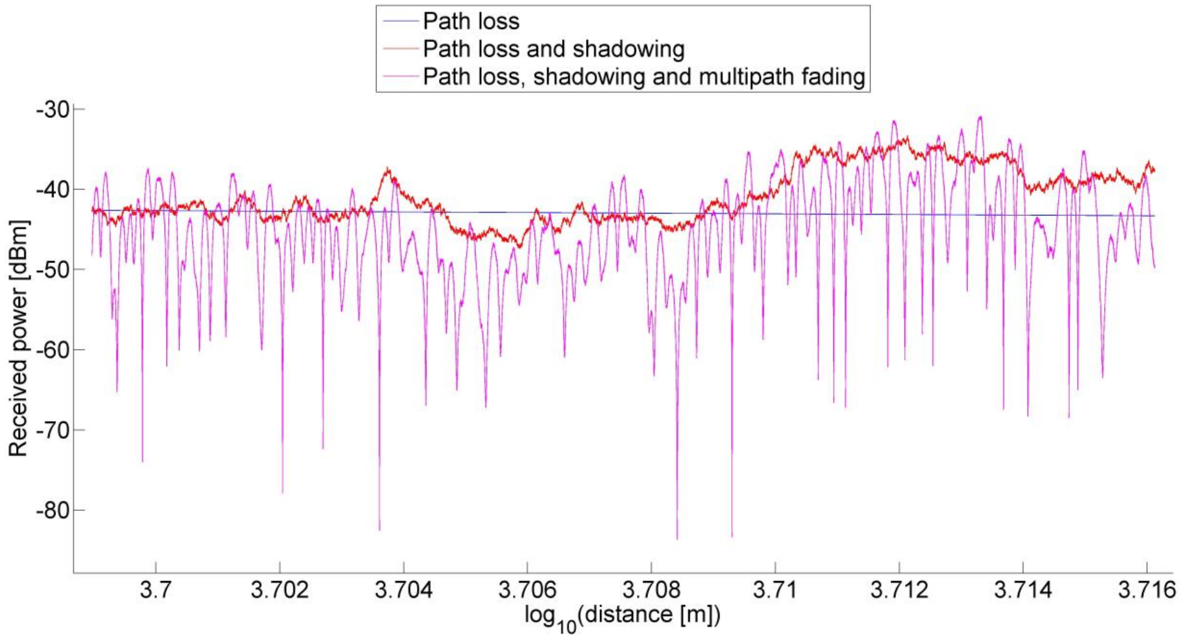

Master's thesis in Signals and Systems

FREDRIK LUNDIN

Department of Signals and Systems
CHALMERS UNIVERSITY OF TECHNOLOGY
Gothenburg, Sweden 2015

REPORT NO. EX018/2015

Modeling of communication channels for analog and digital broadcast reception in cars

Fredrik Lundin

Department of Signals and Systems
CHALMERS UNIVERSITY OF TECHNOLOGY
Göteborg, Sweden, 2015

Modeling of communication channels for analog and digital broadcast reception in cars
FREDRIK LUNDIN

Technical report no EX018/2015
Department of Signals and Systems
Chalmers University of Technology
SE-412 96 Göteborg
Sweden
Fax +46 31 772 17 48
Phone, switchboard +46 31 772 10 00
Göteborg, 2015

The thesis project was performed at the department of Driver Interaction & Infotainment at Volvo Car Corporation, Göteborg.

The figure on the cover page shows three effects that have been studied and that affect the performance of broadcast reception. More details are given in for example section 2 and section 4.

Modeling of communication channels for analog and digital broadcast reception in cars
FREDRIK LUNDIN
Department of Signals and Systems
Chalmers University of Technology

Abstract

The performance of broadcast reception is dependent on several factors. Among these factors are phenomena such as multipath fading, path loss and shadowing. To investigate the performance of a car radio, one method is to use a car and drive in different environments and do recordings of broadcasts in several environments. Then these recordings can be used afterwards for performing measurements. To make this process more efficient, the effects of some environments can be described by mathematical modeling and the effects can be simulated in a computer. In this project, a simulator tool was implemented in which it is possible to apply the mentioned effects to a radio broadcast. The output of that simulator tool can be used for testing of car radios.

The implementation of the simulator tool has been verified in terms of comparisons to theory. The project has had an emphasis on radio broadcasts and in particular the analog FM radio technique. In the simulator tool it is possible to create FM signals from the very beginning while for the digital DAB radio technique, recordings must be loaded into the simulator tool. For FM signals, the user can use a single-frequency tone or contents from an audio file as information.

Since the required time to do the simulations is small in comparison to do testing with a car in some environment, there is a gain in time that can be achieved by using the simulator tool. Thanks to the lower required time, many more cases of for example multipath fading effects can be tested. Testing performed with a car requires some resources in terms of a car, fuel and persons working with the testing. This implies that the implemented simulator tool can have a benefit when it comes to time and money spent on testing of broadcast reception.

Keywords: *multipath fading, path loss, shadowing, radio techniques, cars, simulator tool*

Acknowledgements

During this project I have had the possibility to have support from several persons. It has been very valuable and I would like to thank for this support. More specifically I would like to thank the following persons:

- Claes Lindgren. For spending much time and energy on the project and having a large interest in the progress of the project. For example testing early versions of the simulator tool and reading early versions of the report has been very valuable.

- The group at Volvo Car Corporation at which the project was done and manager Johannes Reesalu. The project has been a good opportunity to learn more within several areas. In addition, it has been inspiring to see and be part of a well performing group having high quality demands and a positive atmosphere.

- Katharina Hausmair. It has been very good to have the possibility to ask many questions about technical parts of the project. It was very good to have the reviews of the report and which I think had a large impact on the quality of the report.

- Taimoor Abbas. It was very good to discuss technical parts of the project and I think that it was good for understanding of technical problems.

Contents

1 Introduction 1
1.1 Context . . . 1
1.2 Background . . . 1
1.3 Aims . . . 2
1.4 Scope . . . 2
1.5 Questions . . . 2
1.6 Method . . . 3
1.7 Thesis outline . . . 3

2 Theory 4
2.1 Radio . . . 4
2.1.1 FM radio . . . 4
2.1.2 DAB radio . . . 7
2.2 Path loss and shadowing . . . 10
2.2.1 Path loss . . . 10
2.2.2 Shadowing . . . 11
2.2.3 Path loss and shadowing combined . . . 13
2.3 Multipath fading . . . 13
2.3.1 Introduction to multipath fading . . . 14
2.3.2 Simulation of local scattering . . . 15
2.3.3 Implementation of time selectivity by Doppler spreading 18
2.3.4 Implementation of frequency selectivity by time spreading . . . 19
2.3.5 Power spectral density and autocorrelation . . . 21
2.3.6 Scaling of channel coefficients . . . 22
2.3.7 Rician fading . . . 26

3 Description of the system 28
3.1 Overview of the simulator tool . . . 28
3.2 Input and output of files . . . 30
3.2.1 URT file . . . 30
3.2.2 Audio file (.mp3) . . . 32
3.2.3 Excel document . . . 33
3.3 FM radio signal generation . . . 33
3.4 Communication channel . . . 35
3.4.1 Multipath fading . . . 36
3.4.2 Path loss and shadowing . . . 37
3.5 Receiver . . . 38

4 Results 39
4.1 FM radio signal generation 39
4.2 Multipath fading 40
4.3 Path loss and shadowing 47

5 Discussion 51
5.1 Limitations 52
5.2 Possible improvements 53
5.3 Suggestions on usage of simulator tool 54

6 Conclusion 54
6.1 Accuracy of model 55
6.2 Time and frequency dependent broadcast reception performance 55
6.3 Environments 55
6.4 Fading models 56
6.5 Same model for analog and digital techniques 56

References 57

A Appendix 60
A.1 Header information for URT file 60
A.2 Excel document with used settings 60

1 Introduction

The thesis project was performed at the department of Driver Interaction & Infotainment at Volvo Car Corporation, Göteborg. This section presents an introduction to the project. For example it is described how the outcome of the project can be used to improve efficiency regarding analysis of broadcast reception performance at Volvo Car Corporation.

1.1 Context

The title of the thesis project is “Modeling of communication channels for analog and digital broadcast reception in cars”. The thesis project covers several types of communication channels by combining several effects that a communication channel can have and by adjustment of the settings of these effects. Since the modeling is made for a car it is especially important to cover effects of the communication channel that have impact on the broadcast reception when the receiver is in movement.

1.2 Background

Using an accurate model which describes the communication channel for analog and digital radio techniques for cars could be an alternative to performing testing of the performance of the signal reception in some environments. Therefore, usage of such model in simulations can reduce the amount of time and money that would have been spent on testing. To perform testing of signal reception would require resources if the testing is done in the way that a car is used in a so called expedition, where it is used to drive in different environments and record broadcasts in these environments. Testing can be performed during the expedition and the recordings can be used several times after the expedition. The recordings can be used to perform measurements. Then these measurements can be used to analyse the performance of broadcast reception. However, to do an expedition requires resources such as planning of the expedition, a car, fuel, persons working with the testing and recordings and so on.

By using an accurate/realistic model, many environments can quickly be created by simulations and the time required to do such simulations is smaller than performing testing in different environments. Simulations created by using a model can easily create many different scenarios of broadcast reception and give control of the settings of the environment. In measurements of a real environment the settings of the environment can only be changed to some extent, e.g. by moving objects in the environment so that the behaviour of reflections will be changed. Such movement of objects can be troublesome but in a simulation it is just to specify the behaviour of e.g. the reflections.

1.3 Aims

The purpose of the thesis is to model communication channels for analog and digital radio techniques for cars with an emphasis on the FM radio technique. The result of the model is expected to give knowledge about how communication channels vary with time and frequency due to e.g. fading[1], the environment and the velocity of the car. For environments in which it may be difficult to communicate, the model could indicate that other communication techniques should be used. Different distances of the communication will imply different types of performance decreasing phenomena, so the model will have to handle path loss, shadowing and multipath fading [5, page 27].

A central part of the thesis was to create an accurate mathematical model which describes communication channels depending on e.g. environment and velocity. It was realised in terms of a simulator tool which is a MATLAB program. This means that the aim of the thesis was to create a simulator tool which relies on an accurate model for communication channels. The focus of the thesis was the Frequency Modulation (FM) [8] radio technique, but the ambition was that the model should enable additions also for digital techniques that could be added after the thesis.

1.4 Scope

The project had an emphasis on the FM radio technique. Digital techniques have also been studied so that the model can enable additions of such techniques. It has been studied if the basis of the model can be the same for analog and digital techniques since it can be useful when adding digital techniques to the model. It is possible to use the Digital Audio Broadcasting (DAB) [6] radio technique to some extent in the simulator tool. Other than that, digital techniques are beyond the scope of this thesis.

1.5 Questions

The following list describes the questions that have been studied during the thesis project:

[1]Fading is the effect of communication reaching the destination by several different ways so that the received signal will consist of several components which could e.g. give an attenuation of the received signal in a destructive way [5, page 69].

- How accurately can a mathematical model describe communication channels for analog and digital broadcast reception?
- How will the performance of the broadcast reception vary with time and frequency depending on e.g. fading, environment and velocity and what is a good way of accurately describing this in the model?
- Which environments are important to include in the model and why?
- Which fading models are relevant in some specific environments for cars in motion and not in motion?
- What are the possibilities for having the same basis of the model for both analog (mainly FM) and digital radio techniques?

1.6 Method

The project started with a study of literature describing relevant areas of the project such as fading, path loss, shadowing and modeling of communication channels. Both analog and digital radio techniques were studied, e.g. to answer the question in section 1.5 about having a common basis for these techniques.

Implementation of the model was done continuously, which enabled a good overview of the status of the project and decreased the probability of having an accurate model which would have been to be too complicated to implement. The iterative way of working method Scrum was used in the project which fits the method of continuous implementation well, because in Scrum, the implementation process can be done stepwise so that the risk can be controlled [10, page 3]. If implementation is not done continuously it could be difficult to control the risk and the example above of the model that may be too complicated to implement is an example of bad control of the risk.

Scrum was also used in order to have the planning in line with the group at Volvo Car Corporation at which the project was done. The time of the project was divided into intervals ("sprints") according to Scrum and the duration of each sprint was two weeks, which is an acceptable duration according to Scrum [10, page 7]. Most of the sprints had at least one "Sprint Goal" [10, page 9-10], which typically were theoretical goals or implementation goals.

1.7 Thesis outline

The thesis report contains six sections. Section 1 presents an introduction to the project including motivation for usage of the model. Section 2 presents theoretical information required for understanding of the implemented system. Section 3 presents a description of the implemented system including explanations of how it works. Section 4 presents results from the implemented system and by using results from the simulator tool, the theory used in the simulator tool is discussed. Section 5 presents a discussion of the project in terms of limitations, suggestions on how to improve the system and suggestions on how to use the system. Section 6 presents the conclusion that could be done after having implemented the simulator tool based on the model.

2 Theory

This section presents theoretical information about the techniques used in the project. This includes information about the analog and digital radio techniques FM respective DAB, path loss, shadowing and multipath fading.

2.1 Radio

This section contains information about the radio techniques FM and DAB. The FM radio technique is used to generate such a signal in the simulator tool while DAB signals can only be loaded into the simulator tool. FM radio signals can also be loaded into the simulator tool. Since FM signals can be created in the simulator tool, the section about FM radio has an emphasis on how to create FM signals. Since recordings are used for DAB radio, the section about DAB radio has an emphasis on how the technique works.

2.1.1 FM radio

Frequency modulation is an analog modulation technique used in FM radio [8]. The frequencies in the interval $[87.5, 108]$ [MHz] are widely used in many countries for FM sound broadcasting [1, page 4 and 5]. To have a separation in frequency of 100 [kHz] or 200 [kHz] between the channels, is common in many countries [1, page 4 and 5]. This separation implies that the channels are to be separated by 100 [kHz] or 200 [kHz] in order to not interfere with each other. The FM technique for modulation is a technique where the transmitted information (e.g. audio) implies variations of the frequency of the carrier wave [8]. This frequency can be a frequency in the previously mentioned interval ranging from 87.5 [Mhz] to 108 [MHz]. An FM signal is given by [8]

$$s_{\mathrm{FM}}(t) = A_c \cos\left(2\pi f_c t + 2\pi K_{\mathrm{VCO}} \int_0^t m(t)\,dt\right) \tag{1}$$

where A_c is an amplitude such that the power of the FM signal $s_{\mathrm{FM}}(t)$ is equal to $A_c^2/2$ if using a $1\,[\Omega]$ resistor, f_c is the carrier frequency, K_{VCO} is a gain of the voltage-controlled oscillator (VCO) that is measured in Hz/V [8] so if a voltage V passes through the VCO the frequency $K_{\mathrm{VCO}} \cdot V$ [Hz] is produced. In (1) $m(t)$ denotes the information that is transmitted [8] and it varies with time t. By using the expression $\cos(\alpha+\beta) = \cos(\alpha)\cos(\beta) - \sin(\alpha)\sin(\beta)$ [7], the expression in (1) can be rewritten as

$$\begin{aligned} s_{\mathrm{FM}}(t) = A_c\Bigg(&\cos(2\pi f_c t)\cos\left(2\pi K_{\mathrm{VCO}} \int_0^t m(t)\,dt\right) - \\ &\sin(2\pi f_c t)\sin\left(2\pi K_{\mathrm{VCO}} \int_0^t m(t)\,dt\right)\Bigg) \end{aligned}$$

and the in-phase carrier $I(t)$ and the quadrature-phase carrier $Q(t)$ are expressed as [7]

$$\begin{cases} I(t) = A_c \cos\left(2\pi K_{\mathrm{VCO}} \int_0^t m(t)\,dt\right) \\ Q(t) = A_c \sin\left(2\pi K_{\mathrm{VCO}} \int_0^t m(t)\,dt\right) \end{cases} . \tag{2}$$

If a sinusoid having amplitude A_m and frequency f_m is used as the transmitted information, i.e. if a sinusoid of the form $m(t) = A_m \cos(2\pi f_m t)$ is used, the FM signal can be rewritten [8]. This is because the integral can be easily evaluated as $\big(A_m/(2\pi f_m)\big)\sin(2\pi f_m t)$, which gives the following expression of the FM signal:

$$s_{\mathrm{FM}}(t) = A_c \cos\left(2\pi f_c t + \frac{K_{\mathrm{VCO}} A_m}{f_m}\sin(2\pi f_m t)\right) \tag{3}$$

where the term $K_{\mathrm{VCO}} A_m$ is called frequency deviation and will be denoted as Δf [8]. It can be emphasised that A_m is the maximum amplitude that the sinusoid $A_m \cos(2\pi f_m t)$ will have and if the maximum amplitude of the information is 1, it holds that $\Delta f = K_{\mathrm{VCO}}$. This will be relevant when using other messages than a sinusoid. More specifically it is relevant in the simulator tool when an audio file is loaded into the simulator tool in terms of a .mp3 file because then the loaded audio signal will have at most an absolute value equal to 1. This means that in the case of a maximum amplitude of 1, the expressions in (2) can be written as

$$\begin{cases} I(t) = A_c \cos\left(2\pi\Delta f \int_0^t m(t)\, dt\right) \\ Q(t) = A_c \sin\left(2\pi\Delta f \int_0^t m(t)\, dt\right) \end{cases} . \tag{4}$$

In the implementation, $A_c = 1$ was used and a scaling of the amplitude is done later in the case of generation of FM signals (see section 3.1). According to [1, page 4 and 5] a frequency deviation $\Delta f = 75\,[\text{kHz}]$ is widely used in many countries but $\Delta f = 50\,[\text{kHz}]$ can also be used. Therefore, in the implementation, these two values are available for Δf.

Stereo audio The contents of the left channel and the right channel can be combined to create a stereo audio signal [8]. Channel here implies the audio channel which can be thought of as left and right speaker if using speakers for the audio. If $L(t)$ represents the left channel and $R(t)$ represents the right channel, a stereo signal can be given by writing the information $m(t)$ as [8]

$$m(t) = 0.45\big(L(t) + R(t)\big) + 0.10\cos\left(2\pi \cdot 19 \cdot 10^3 \cdot t\right) + 0.45\big(L(t) - R(t)\big)\cos\left(2\pi \cdot 38 \cdot 10^3 \cdot t\right) \tag{5}$$

where the digital information modulated around 57 [kHz] used in Radio Data System (RDS) is not included. It is not included because RDS will not be used in this project. In (5), the numbers 0.45 and 0.10 are examples of representations of the modulation levels [8]. This means that if $L(t) + R(t) = 2$, the modulation used for $L(t) + R(t)$ is $0.45 \cdot 2 \cdot 75 \cdot 10^3\,[\text{kHz}]$ if $\Delta f = 75 \cdot 10^3\,[\text{kHz}]$ is used as frequency deviation. The sinusoid at 19 [kHz] is called pilot tone [8]. The pilot tone is used by the receiver so that for example a 38 [kHz] signal can be created in the receiver by doubling the pilot tone's frequency [8]. Thereby the information $L(t) - R(t)$ around 38 [kHz] can be found.

In the simulator tool, the MATLAB function `audioread` has been used to load the audio data into the simulator tool. It gives a matrix $\mathbf{S}$ which in the case of two audio channels contains all the audio information as a matrix having N rows and two columns, where N is the number of samples [16]. Except for section 2.1.2, the time t will be replaced by nT_s in the rest of the report. The integer n, $n = 0, 1, ..., N-1$, where N is the number of samples, is used to denote a sample. The integer n has the property that the time t will be sampled at even intervals according to $t = nT_s = n/f_s$, where $T_s = 1/f_s$ is the time between two samples and f_s is the sampling frequency. The elements in the columns of $\mathbf{S}$ are $L(nT_s)$ and $R(nT_s)$ for different times nT_s. The matrix $\mathbf{S}$ has the structure

$$\mathbf{S} = \begin{bmatrix}\mathbf{l} & \mathbf{r}\end{bmatrix}$$

where $\mathbf{l}$ and $\mathbf{r}$ are column vectors containing $L(nT_s)$ respectively $R(nT_s)$ for all times nT_s. The matrix $\mathbf{S}$ is scaled giving a new matrix $\hat{\mathbf{S}}$. The matrix $\hat{\mathbf{S}}$ will have elements $\hat{s}_{ij}$, $i = 1, 2, ..., N$, $j = 1, 2$, where i is an index of a row and j is an index of a column in $\hat{\mathbf{S}}$. The scaling is performed according to

$$\hat{s}_{ij} = \frac{1}{\max_{i,j}|s_{ij}|} s_{ij}$$

where s_{ij} are the elements of $\mathbf{S}$ and $|s_{ij}|$ denotes absoute value of s_{ij}. The maximum absolute value of an element in $\hat{\mathbf{S}}$ is 1. The elements of $\hat{\mathbf{S}}$ can be denoted as $\hat{L}(nT_s)$ and $\hat{R}(nT_s)$ and these elements will be used in (5).

An example in which $L(nT_s) = R(nT_s)$, $\forall\, nT_s$ can be considered. The fact that $L(nT_s) = R(nT_s)$, $\forall\, nT_s$ will imply that $\hat{L}(nT_s) = \hat{R}(nT_s) = 1$, $\forall\, nT_s$ since $\hat{\mathbf{S}}$ will only contain ones at all positions. This means that the summation signal $\hat{L}(nT_s) + \hat{R}(nT_s) = 2$, $\forall\, nT_s$ and the modulation level of the summation signal will be $0.45 \cdot 2 = 0.90$ for all times nT_s. The pilot tone has a modulation level of 0.10 when the sinusoid is equal to 1. Together with the fact that the difference signal $L(nT_s) - R(nT_s) = 0$, $\forall\, nT_s$, this means that the total modulation level is at most $0.90 + 0.10 + 0.00 = 1.00$. This number corresponds to the maximum amplitude of the audio signal. As was previously mentioned, if $A_m = 1$, a frequency deviation of 75 [kHz] will be used. That the summation signal has a modulation level of 0.90 and that the difference signal has a modulation level of 0.00 is reasonable. Since the both audio channels are equal it implies that the difference signal is zero and therefore there is no point in using any modulation for this signal. This means that all the modulation goes to the summation signal.

2.1.2 DAB radio

DAB is a digital radio system that is good at handling reception when the receiver is in movement (as a car may be) and multipath fading effects [6]. These two properties make the technique interesting to study in this thesis project since a receiver in movement and multipath fading are very central parts of the project.

DAB uses a modulation called COFDM (Coded Orthogonal Frequency Division Multiplexing), which can handle multipath fading effects in a good way [11, page 1]. In fact, the DAB system had an emphasis on reception problems for cars in movement in its design and in particular there was an emphasis on multipath fading effects [11, page 2]. This section about DAB radio will explain the techniques in the term "Coded Orthogonal Frequency Division Multiplexing" so that the differences compared to the FM radio technique can be seen.

Error coding (C) The term "Coded" in COFDM is a short term for error coding [11, page 2]. The error coding can be used to achieve a low bit-error ratio (BER) at a low signal-to-noise ratio (SNR) [11, page 6] and this decrease in required SNR can be a motivation for using error coding.

Orthogonality (O) According to [11, page 3] a frequency spacing of carriers can be defined as $f_{\text{symbol}} = 1/T_{\text{symbol}}$ where T_{symbol} is an integration period in the receiver related to the useful content of a symbol [11, page 3 and 4]. According to [11, page 3] a baseband carrier $x_k(t)$ can be defined to be

$$x_k(t) = e^{j2\pi f_{\text{symbol}} kt} = e^{j\frac{2\pi}{T_{\text{symbol}}} kt}$$

where k indicates that it is baseband carrier number k. To show that two baseband carriers $x_k(t)$ and $x_l(t)$ are orthogonal, the integral $\int_\tau^{\tau+T_{\text{symbol}}} x_k(t) x_l^*(t)\, dt$ is to be evaluated [11, page 3], where τ is a delay that can vary and * represents complex conjugate. The delay τ can vary within the interval $[0, t_{\max} - T_{\text{symbol}}]$ where $t_{\max}$ is the maximum value for the time t. Evaluating the integral gives

$$\int_\tau^{\tau+T_{\text{symbol}}} x_k(t) x_l^*(t)\, dt = \int_\tau^{\tau+T_{\text{symbol}}} e^{j\frac{2\pi}{T_{\text{symbol}}} kt} e^{-j\frac{2\pi}{T_{\text{symbol}}} lt}\, dt = \int_\tau^{\tau+T_{\text{symbol}}} e^{j\frac{2\pi}{T_{\text{symbol}}} (k-l)t}\, dt. \quad (6)$$

By using that $e^{jx} = \cos(x) + j\sin(x)$ [21] and dividing the integral into two integrals, the integral can be written as

$$\int_\tau^{\tau+T_{\text{symbol}}} \cos\left(\frac{2\pi}{T_{\text{symbol}}}(k-l)t\right) dt + j\sin\left(\frac{2\pi}{T_{\text{symbol}}}(k-l)t\right) dt = \int_\tau^{\tau+T_{\text{symbol}}} \cos\left(\frac{2\pi}{T_{\text{symbol}}}(k-l)t\right) dt + j\int_\tau^{\tau+T_{\text{symbol}}} \sin\left(\frac{2\pi}{T_{\text{symbol}}}(k-l)t\right) dt. \quad (7)$$

The integrals over the two sinusoids will be equal to zero if $k \neq l$. Since the sinusoids are periodic having the period $T_{\text{symbol}}/(k-l)$ and k and l are integers, the sinusoids will have an integer number of periods during T_{symbol}. However, if $k = l$ the following holds:

$$\begin{cases} \int_{\tau}^{\tau+T_{\text{symbol}}} \cos\left(\frac{2\pi}{T_{\text{symbol}}}(k-l)t\right) dt = \int_{\tau}^{\tau+T_{\text{symbol}}} 1\, dt = T_{\text{symbol}} \\ j \int_{\tau}^{\tau+T_{\text{symbol}}} \sin\left(\frac{2\pi}{T_{\text{symbol}}}(k-l)t\right) dt = j \int_{\tau}^{\tau+T_{\text{symbol}}} 0\, dt = 0 \end{cases} . \tag{8}$$

By combining (6), (7) and (8) it is seen that the following holds:

$$\int_{\tau}^{\tau+T_{\text{symbol}}} x_k(t) x_l^*(t)\, dt = T_{\text{symbol}} \delta[k-l]$$

where δ is the Kronecker delta having the property that [22]

$$\delta[k-l] = \begin{cases} 1, \; k = l \\ 0, \; \text{else} \end{cases} .$$

The described orthogonality property of the baseband carriers is what is meant by “Orthogonality” in COFDM [11, page 2 to 4]. The orthogonality property of COFDM is important and is a key of the last property of COFDM, the Frequency Division Multiplexing (FDM) property.

Frequency Division Multiplexing (FDM) COFDM uses multiple carriers for the transmission of data [11, page 2] in contrast to FM which only uses one carrier for the transmission. Multiple carriers are used to improve the communication when there is multipath fading because if only one carrier is used and the delay time between the paths is long enough relative to the time of a symbol, the transmitted symbols will interfere with each other which leads to the inter-symbol interference (ISI) phenomenon [11, page 2]. To explain delay time, an example can be considered. Two symbols are transmitted at two different times and there are two paths that the symbols can pass at their way to the receiver. Figure 1 describes the scenario of transmission, paths and symbol reception.

According to Figure 1, the received symbols will arrive at three different times. If these times are denoted as t_3, t_4 and t_5, the relation between times of symbol reception and received symbols is

$$\begin{cases} t_3 = 10\,[\mu\text{s}] : \; s'_{11} \\ t_4 = 15\,[\mu\text{s}] : \; s'_{21} \text{ and } s'_{12} \\ t_5 = 20\,[\mu\text{s}] : \; s'_{22} \end{cases}$$

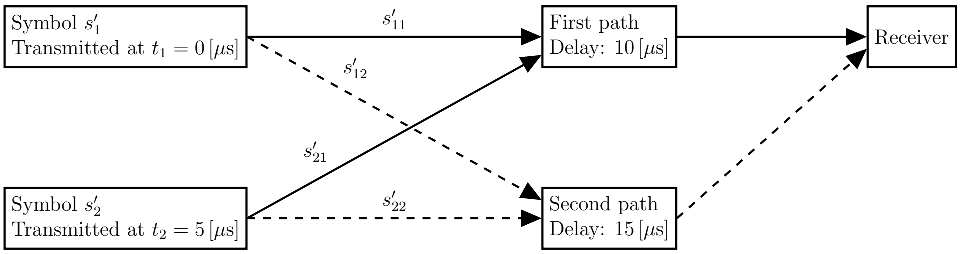

Figure 1: Example of delay time. The solid arrows are related to the first path and the dashed arrows are related to the second path.

where s'_{ij}, $i, j = 1, 2$ is the symbol i received through path j. So at time t_4, the symbols will interfere with each other, i.e. ISI will occur. Since the symbol s'_1 was receieved through the first path at time t_3 and through the second path at time t_4, the delay between the paths is $t_4 - t_3 = 5\,[\mu s]$.

The ISI can be reduced by transmitting the symbols at a slower rate [11, page 2]. However, this can be inefficient because the rate of the received information will decrease and the rate with which information arrives at the receiver may not be high enough and the decrease is therefore perhaps not an alternative. In the example related to Figure 1, this decrease in rate would correspond to increasing t_2 to for example $15\,[\mu s]$. Then the ISI potentially introduced by the two paths would be avoided.

It can be emphasised that the problem of potentially having ISI will still remain when having multiple carriers. Instead of having one carrier having the requirement of not transmitting too slowly, all the multiple carriers can transmit at a slower rate and if the transmissions are done slowly enough there will not be any ISI [11, page 2 and 3]. If the number of carriers that transmits slowly is large enough, the rate with which the receiver can receive information can be the same as if having one carrier that transmits quickly. This usage of multiple carriers and thereby multiple streams containing information implies the “Frequency Division Multiplexing” in COFDM [11, page 2 and 3].

2.2 Path loss and shadowing

This section presents information about path loss and shadowing and how these effects are combined in the simulator tool.

2.2.1 Path loss

The definition of path loss in a linear scale is the ratio between the transmitted power $P_{\text{transmitted}}$ and the received power P_{received}, i.e. the ratio $P_{\text{transmitted}}/P_{\text{received}}$

and in dB this corresponds to $10\log_{10}(P_{\text{transmitted}}/P_{\text{received}})$ which is defined as the path loss [5, page 31]. Typically the received power is smaller than the transmitted power giving a dB value of the path loss larger than zero [5, page 31].

According to [5, page 46], it can be sufficient to use simple models for path loss since it can be difficult to find a model which can describe the path loss accurately in several environments. A model for the loss in power given by path loss is [5, page 46]

$$P_{\text{received}} = P_{\text{transmitted}} K \left(\frac{d_0}{d}\right)^{\gamma} \tag{9}$$

where K is a constant, d is distance, d_0 is a reference distance related to the antenna far field and γ is path-loss exponent. One example of the constant K is the following [5, page 47]:

$$K\,[\text{dB}] = 20\log_{10}\frac{\lambda}{4\pi d_0}$$

where λ is the signal wavelength and K is the free-space path gain if omnidirectional antennas are assumed [5, page 32, 46 and 47]. A typical assumption regarding the reference distance d_0 is to use a d_0 in the interval $[10, 100]$ [m] for transmission outdoors [5, page 47] which will typically be the case for this project. The loss in power in (9) can be written as [5, page 46]

$$P_{\text{received}}\,[\text{dBm}] = P_{\text{transmitted}}\,[\text{dBm}] + K\,[\text{dB}] - 10\gamma\log_{10}\left(\frac{d}{d_0}\right) \tag{10}$$

where dBm is a unit of power which is calculated as $10\log_{10}(P/0.001)$ for a power P [5, page 32] meaning that 1 [mW] is equal to 0 [dBm].

In [5, page 47] some typical values of path-loss exponents γ are given. For example a $\gamma \in [3.7, 6.5]$ is mentioned for "urban macrocells" and a $\gamma \in [1.6, 3.3]$ for a factory. A macrocell is a cell in which a cell base station can provide coverage of some square miles when positioned at a high position and transmitting with very high power [5, page 9]. The information about the large area is relevant for this project because the distance between the transmitter and the car is assumed to always be relatively large.

2.2.2 Shadowing

If there are objects between the transmitter and the receiver (car in this case), the received power will typically vary randomly [5, page 48]. It can be mentioned that also reflecting surfaces and scattering objects can change which will imply randomness in the attenuation [5, page 48]. Since for example the size and the position of the objects between the transmitter and the receiver can be unknown and since the changes regarding reflecting surfaces and scattering objects can also be unknown, statistics is used to model these effects [5, page 48]. The most common such statistical model is log-normal shadowing which has shown good performance both outdoors and indoors [5, page 48]. In log-normal shadowing, the parameter $\psi = P_{\text{transmitted}}/P_{\text{received}}$ is said to follow a log-normal distribution [5, page 48]. In a dB scale, the parameter ψ follows a Gaussian distribution with mean $\mu_{\psi_{\text{dB}}}$ and standard deviation $\sigma_{\psi_{\text{dB}}}$ [5, page 49]. If the transmission is performed outdoors, a standard deviation $\sigma_{\psi_{\text{dB}}} \in [4, 13]$ [dB] can be appropriate to use as it is supported by most empirical studies [5, page 50].

In [2, page 3948], shadow fading $s[k]$ given by objects blocking the propagation follows a log-normal distribution and is modeled as a first-order autoregressive process according to the expression

$$s[k+1] = e^{-\frac{vT_s}{X_c}} s[k] + n[k] \tag{11}$$

where T_s is the sampling period, X_c is the effective decorrelation distance, v is the velocity and $n[k]$ represents white Gaussian noise having mean value zero and variance $\sigma_n^2 = \left(1 - e^{-2vT_s/X_c}\right)\sigma_s^2$, where σ_s is the log-standard deviation of the shadow fading process. In [5, page 51] it is mentioned that the decorrelation distance X_c can be in the same order of size as a blocking object and that $X_c \in [50, 100]$ [m] can be typical values outdoors. At the decorrelation distance X_c, the covariance of the shadow fading will be equal to $1/e$ of the maximum value [5, page 51]. So the interpretation of the decorrelation distance is that when the receiver has moved X_c [m] away from a point P, the shadow fading at the new point has a certain similarity to the shadow fading at the point P. This similarity is equal to $1/e$ of the maximum covariance.

The autocorrelation function for the described shadow fading process in (11) is [2, page 3948]

$$R_s[k] = \sigma_s^2 e^{-|k|\frac{vT_s}{X_c}}. \tag{12}$$

Several points can be made regarding (11) and (12). In (11) it can be seen that the noise $n[k]$ is the input to the shadow fading process and is therefore what gives “energy” to the process. It can be seen that the shadow fading at the next sample instance $(k+1)$ is dependent on the shadow fading at the current sample instance (k), i.e. the shadow fading process has correlation. It can be seen in (12) that this correlation is dependent on several factors. If the car moves with a high velocity v the shadow fading will decorrelate quickly which is reasonable because then the decorrelation distance X_c is reached quickly. If the sampling frequency f_s is high such that the sampling period $T_s = 1/f_s$ is low, more samples will be required to describe the decorrelation. The value of the autocorrelation at the decorrelation distance can be given from (12) by using $|k|\,[\text{samples}] \cdot v\,[\text{m/s}] \cdot T_s\,[\text{s/sample}] = X_c\,[\text{m}]$. Then it can be seen that $R_s[k] = (1/e)\sigma_s^2$ is $1/e$ of its maximum value.

The shadowing was implemented by filtering the white Gaussian noise through a filter defined by (11) and the filtering was done with the MATLAB function `filter` [17].

2.2.3 Path loss and shadowing combined

When shadowing is to be added to path loss, the following model is presented in [5, page 51]:

$$\frac{P_{\text{received}}}{P_{\text{transmitted}}}\,[\text{dB}] = 10\log_{10}K - 10\gamma\log_{10}\frac{d}{d_0} - \psi_{\text{dB}}$$

where ψ_{dB} follows a Gaussian distribution with mean value zero and variance $\sigma^2_{\psi_{dB}}$ as was previously described. Rewriting this to the form of (10) gives

$$P_{\text{received}}\,[\text{dBm}] = P_{\text{transmitted}}\,[\text{dBm}] + K\,[\text{dB}] - 10\gamma\log_{10}\left(\frac{d}{d_0}\right) - \psi_{\text{dB}}$$

and this is the model that has been used in the simulator tool.

2.3 Multipath fading

This section describes techniques for simulation of multipath fading channels. The term fading means that the received signal consists of several components where each component has experienced a different path on its way to the receiver and may have some delay τ (time) [5, page 69]. The definition of delay used in this thesis is the following. If the signal consists of two components which arrive at times $t_1 = 10\,[\mu\text{s}]$ and $t_2 = 15\,[\mu\text{s}]$, the second component has a delay relative to the first component. This delay is $5\,[\mu\text{s}]$. These path delays can in the case when $f_c\tau \gg 1$ (where f_c is the carrier frequency [5, page 65]) give large changes of the phase of the components which can imply that the received signal can be attenuated quickly [5, page 69].

According to [5, page 29] it can be difficult to accurately model the channel in a deterministic way so instead statistical models can be used to represent the channel. Two such random representations will be presented in this section and the names of these representations are Rayleigh and Rician where the Rayleigh fading channel representation can be used for paths which are not line-of-sight and the Rician fading channel representation can be used for paths which are line-of-sight [12].

2.3.1 Introduction to multipath fading

Figure 2 shows the principle of multipath fading where the transmitted information can reach the receiver via several paths. As was mentioned in section 2.3 the line-of-sight communication (direct path) can be represented by a Rician fading channel and the paths that have a reflection can be represented by a Rayleigh fading channel. The figure also shows local scattering which happens close to the car and can be represented by many reflections [12]. The reflections that do not happen close to the car (one per path except for the direct path) will give a delay and it is the many reflections that happen close to the car (for each path) that will give the multipath fading [12]. To summarise, the following holds:

$$\begin{cases} \text{Rician fading path: line-of-sight + local scattering} \\ \text{Rayleigh fading path: local scattering} \end{cases}$$

and in the case of Rayleigh fading, the reflections that do not happen close to the car will introduce delays of the received components [12]. When path is mentioned in this thesis it refers to long paths as in Figure 2 having no reflection or one reflection (i.e. all the reflections that happen in the local scattering are not paths).

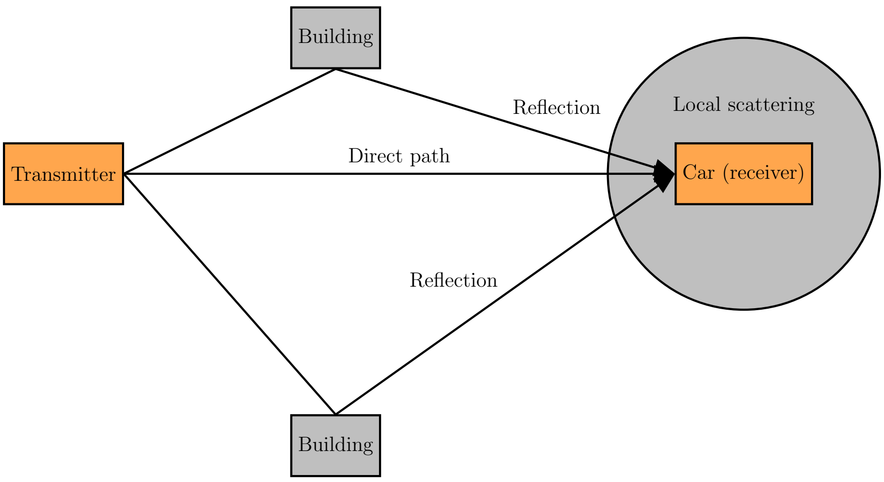

Figure 2: Three communication paths and local scattering.

It can be seen in Figure 2 that the distances for the different paths vary. Since the speed of the communication is the same for all paths, the time (time = distance/speed) that it takes for the information to reach the car will vary and a delay τ between the paths will be introduced. If the difference in distance for the paths is such that $f_c\tau \gg 1$ there will be quick attenuations of the received signal.

2.3.2 Simulation of local scattering

According to [9, page 1] a model called Clarke's model is common to use for representation of flat fading in e.g. urban environments. Clarke's model is used to simulate local scattering. Since this section only describes information about local scattering, the section only deals with Rayleigh fading paths. However, as was mentioned in section 2.3.1, local scattering is a component of Rician fading paths as well. More information about Rician fading paths is given in section 2.3.7.

Flat fading is equivalent to the expression frequency-flat fading. Frequency-flat fading implies that the receiver can not distinguish between the paths so the receiver will experience it as only one path [9, page 2]. The interpretation of frequency-flat fading is that all frequencies will be affected by the fading in the same way.

The used model makes some assumptions of the communication and these assumptions are [9, page 1]:

- Fixed transmitter
- Vertically polarized transmit antenna
- Mobile terminal

The assumption about the mobile terminal will be valid for a moving car and it is reasonable to assume that the transmitter does not move. However, it can be good to remember that the model assumes vertical polarization because if the receiver does not use this, the model will most likely lose some accuracy. The electric field $E_{\text{received}}(nT_s)$ that is received at the antenna of the mobile terminal has L numbers of azimuthal plane waves/scatterers [9, page 1] for each path. This means that for each path, the received plane waves have experienced L different ways and therefore L different levels of fading. In this thesis, ways represent reflections in the local scattering while paths represent single reflections that do not happen in the local scattering or it can represent a direct path. The received electric field for one path can be expressed by [9, page 1]

$$E_{\text{received}}(nT_s) = \sum_{l=1}^{L} \bar{E}_l C_l \cos\big(2\pi f_c nT_s + \theta_l(nT_s)\big) \tag{13}$$

where $\bar{E}_l$ can be replaced by $\bar{E}$ because $\bar{E}_l$ is assumed to have a constant value for all L plane waves and C_l is a random variable describing the fading experienced on the lth way to the receiver, having the property that the statistical expectation $E\big[\sum_{l=1}^{L} C_l^2\big]$ is equal to 1 [9, page 1]. In the local scattering, there can be many ways to the receiver and the exact number of ways is L. In [9], it is not expressed explicitly what $\bar{E}_l$ is, but it is mentioned that the L plane waves have the same average amplitude [9, page 1]. Therefore it is likely that $\bar{E}_l = \bar{E}$ is the average amplitude or just amplitude of each plane wave. By using the information that the phases $\theta_n(nT_s) = 2\pi f_l nT_s + \phi_l$, where f_l is the Doppler shift of the wave with index l and ϕ_l are arbitrary carrier phases [9, page 1], (13) can be rewritten as

$$E_{\text{received}}(nT_s) = \sum_{l=1}^{L} \bar{E} C_l \cos(2\pi f_c nT_s + 2\pi f_l nT_s + \phi_l). \tag{14}$$

Therefore the received electric field is dependent on the Doppler shift. The Doppler shift is dependent on the carrier wavelength λ, with which arbitrary azimuthal angle α_l the wave is received and the velocity v according to the relationship [9, page 1]

$$f_l = \frac{v\cos(\alpha_l)}{\lambda}.$$

If the carrier wavelength is approximated as $\lambda \approx c/f_c$ where $c = 3 \cdot 10^8$ [m/s] represents the speed of light when going through free space [9, page 1] the Doppler shift can be written as $f_l = v f_c \cos(\alpha_l)/c$. If the arbitrary azimuthal angle α_l is zero, the Doppler shift will be $f_l = v f_c/c$ and this is called the maximum Doppler shift [9, page 10]. In the rest of the report, the maximum Doppler shift will be denoted as f_d and this notation can be found in for example [9, page 1].

It can be mentioned that the motion that gives a Doppler shift is a relative motion [12] but due to the assumptions mentioned above with a fixed transmitter and a mobile terminal/car, the velocity is determined totally by the velocity of the car. When the maximum Doppler shift is created it means that the scattering components that are reflected close to the car have a direction that is opposite to the one of the car [12] which should happen exactly when a component is reflected in front of the car and then getting the direction towards the car.

The summation in (14) can via usage of the previously defined $\theta_l(nT_s)$ be rewritten as [9, page 1]

$$E_{\text{received}}(nT_s) = \underbrace{\bar{E}\sum_{l=1}^{L} C_l \cos\big(\theta_l(nT_s)\big)}_{\text{In-phase component, } I(nT_s)} \cos(2\pi f_c nT_s) - \underbrace{\bar{E}\sum_{l=1}^{L} C_l \sin\big(\theta_l(nT_s)\big)}_{\text{Quadrature component, } Q(nT_s)} \sin(2\pi f_c nT_s).$$

The central limit theorem implies that if the number of plane waves L is large, the in-phase component and the quadrature component (which are uncorrelated) of the received electric field will be normally distributed [9, page 1]. These components will have mean 0 and variance $\Omega/2 = \sigma^2$ [9, page 1]. The absolute value of the received field (also called envelope) will become $|E_{\text{received}}(nT_s)| = \sqrt{I^2(nT_s) + Q^2(nT_s)}$ and this absolute value is Rayleigh-distributed [9, page 1].

Since $I(nT_s)$ and $Q(nT_s)$ are orthogonal, the complex number $c(nT_s) = I(nT_s) + jQ(nT_s)$ can be used to represent the received electric field at each time nT_s. Since the carrier frequency f_c is not involved in $c(nT_s)$, this representation is valid at a baseband level. This is also supported by [5, page 78] which uses a similar complex number as a lowpass representation of the received signal. In this thesis, the complex number $c(nT_s)$ will represent so called channel coefficients which describe how the channel will imply changes to the received signal's amplitude and phase. Since the channel coefficients were derived related to flat multipath fading caused by local scattering, they can also be said to represent flat multipath fading channel coefficients. In fact, since the envelope of the channel coefficients, which is $|c(nT_s)|$, is Rayleigh-distributed, $c(nT_s)$ can be used to describe a Rayleigh fading channel. Now the question is how to generate the normally distributed $I(nT_s)$ and $Q(nT_s)$ in a good way and an explanation of this follows.

A normal distribution is sometimes called to be a Gaussian distribution [24] and therefore in what follows the term Gaussian equals the term normal. In [3, page 3] it is said that the complex Gaussian process $\mu(nT_s)$ which is defined as

$$\mu(nT_s) = \mu_1(nT_s) + j\mu_2(nT_s) \tag{15}$$

and which consists of two narrowband real Gaussian processes having mean zero and the same variance σ^2 is an often used model for randomness in the complex equivalent baseband. In [3, page 4] it is said that the Gaussian processes $\mu_1(nT_s)$ and $\mu_2(nT_s)$ can be constructed by the sum of an infinite number of sinusoids according to

$$\mu_i(nT_s) = \lim_{L_i \to \infty} \sum_{l=1}^{L_i} c_{i,l} \cos(2\pi f_{i,l} nT_s + \theta_{i,l}) \tag{16}$$

where $i = 1, 2$ [3, page 3], the phase $\theta_{i,l}$ is uniformly distributed in $(-\pi, \pi]$, $c_{i,l} = 2\sqrt{\Delta f_i \cdot S_{\mu_i \mu_i}(f_{i,l})}$ denotes the gain for the real respective imaginary part and for a specific wave l and $f_{i,l} = l\Delta f_i$ denotes a discrete Doppler frequency for index (i, l). The term Δf_i is selected such that the whole frequency interval that is interesting is covered by the discrete Doppler frequencies and it has the property that $\Delta f_i \to 0$ if the number of sinusoids $L_i \to \infty$ [3, page 4]. This implies that Δf_i is similar to resolution in frequency domain. In [9, page 3] the same expression can be found but with a slightly different interpretation of $c_{i,l}$.

The expression in (16) is an essential part in generating the multipath fading channel coefficients. However, a limited number of sinusoids L_i is used in the implementation since it is not possible to implement (16) exactly in a computer [3, page 4]. A problem with the model that has been explained in this section is that it will give frequency-flat fading. When the receiver can distinguish between the paths the channel has frequency-selective fading [9, page 2]. This is the case that is wanted because it will give correct representation of the channel in environments that have this property. For example in Figure 2 the correct representation would be three paths if the fading requirement $f_c\tau \gg 1$ is assumed to be valid for each path. The interpretation of frequency-selective fading is that in contrast to frequency-flat fading, the fading will affect different frequencies in a different way. Several paths can lead to this effect.

To simulate the frequency-selective property of the channel, time spreading has to be done [9, page 1 and 2] and by using Doppler spreading a property of the channel which implies time selectivity must be simulated [9, page 1].

2.3.3 Implementation of time selectivity by Doppler spreading

By performing Doppler spreading, the channel coefficients will be created. The implemented method for simulating fading channel coefficients is a method which implements (16) for a limited number of sinusoids L_i. For each i and l the phase $\theta_{i,l}$ in (16) is a random sample from a uniform distribution taking values in the interval $(-\pi, \pi]$. The gains $c_{i,l}$ have been calculated according to [3, page 5] as $c_{i,l} = \sigma\sqrt{2/L_i}$, where σ^2 is the variance for both the real and imaginary Gaussian processes [3, page 3] and where the number of sinusoids L_i is different for the real and imaginary part [3, page 5]. The number of sinusoids is calculated as [3, page 5]

$$\begin{cases} L_1 = L_1 \\ L_2 = L_1 + 1 \end{cases} .$$

Since the variance σ^2 is a constant for all i and l it has been set to be 1 and a correction for the amplitude has been done later instead (see section 2.3.6 for more details). This means that the gains that were used in this stage were

$$c_{i,l} = \sqrt{\frac{2}{L_i}}.$$

The discrete Doppler frequencies $f_{i,l}$ can be calculated as [3, page 5]

$$f_{i,l} = f_{\max} \sin\left(\frac{\pi}{2L_i}\left(l - \frac{1}{2}\right)\right)$$

where $f_{\max}$ is the maximum Doppler frequency [3, page 3] which was defined previously as (the maximum Doppler shift) $f_d = vf_c/c$.

2.3.4 Implementation of frequency selectivity by time spreading

According to [9, page 3] the tapped-delay-line channel model is popular for creating the multipath components that the receiver can distinguish between. As was mentioned in section 2.3.2 this will lead to frequency-selective fading. In the tapped-delay-line channel model the delay and time dependent impulse response of the channel having low-pass character is defined as [9, page 3]

$$\tilde{c}\big(\tau(nT_s)T_s, nT_s\big) = \sum_{k=1}^{K(nT_s)} \tilde{c}_k\big(\tau_k(nT_s)T_s, nT_s\big)\delta\Big(\big(\tau - \tau_k(nT_s)\big)T_s\Big) \qquad (17)$$

where $K(nT_s)$ defines the number of paths, $\tilde{c}_k\left(\tau_k(nT_s), nT_s\right),\ k = 1, 2, ..., K(nT_s)$ are the complex channel coefficients which have low-pass character and $\tau_k(nT_s)$ is the delay for the path k [9, page 3 and 4]. The integer k represents an index of a path. The time dependency of $K(nT_s)$ means that the number of paths can change over time and the time dependency of $\tau_k(nT_s)$ means that the delays can change over time. In (17), the delays τ and $\tau_k(nT_s)$ are multiplied with T_s so that the delays represent time delays. For the purpose of making the implementation easier the number of paths does not change over time, i.e. $K(nT_s) = K$ is constant and the delays do not change over time, i.e. $\tau_k(nT_s) = \tau_k$ are constant. The modeling of the channel is done at baseband level. A baseband model is compatible with an instrument that has been used in the project. This is because the instrument expects a baseband signal and then it will handle the upconversion when passing the signal to a radio. The complex channel coefficients are calculated as $\tilde{c}_k(\tau_k T_s, nT_s) = c_k(nT_s)e^{-j2\pi f_c \tau_k T_s}$ [9, page 3 and 4] and $c_k(nT_s)$ is assumed to be the time dependent Gaussian process in (15). It can be emphasised that (15) is used for each path k.

Having an input (signal) $\tilde{s}(nT_s)$ with low-pass character as input to the channel, the output $\tilde{y}(nT_s)$ (also having low-pass character) is given as [9, page 4]

$$\tilde{y}(nT_s) = \sum_{k=1}^{K} \tilde{c}_k(nT_s)\tilde{s}\big((\tau - \tau_k)T_s\big),\ n = 0, 1, ..., N-1 \tag{18}$$

where N is the number of samples. With some inspiration from Fig.1 in [9, page 4], Figure 3 shows the principle of the tapped-delay-line channel model. The complex channel coefficients are represented as $\tilde{c}_k(nT_s)$, $k \in \{1, 2, K\}$ to save some space. The figure shows how the output $\tilde{y}(nT_s)$ is calculated.

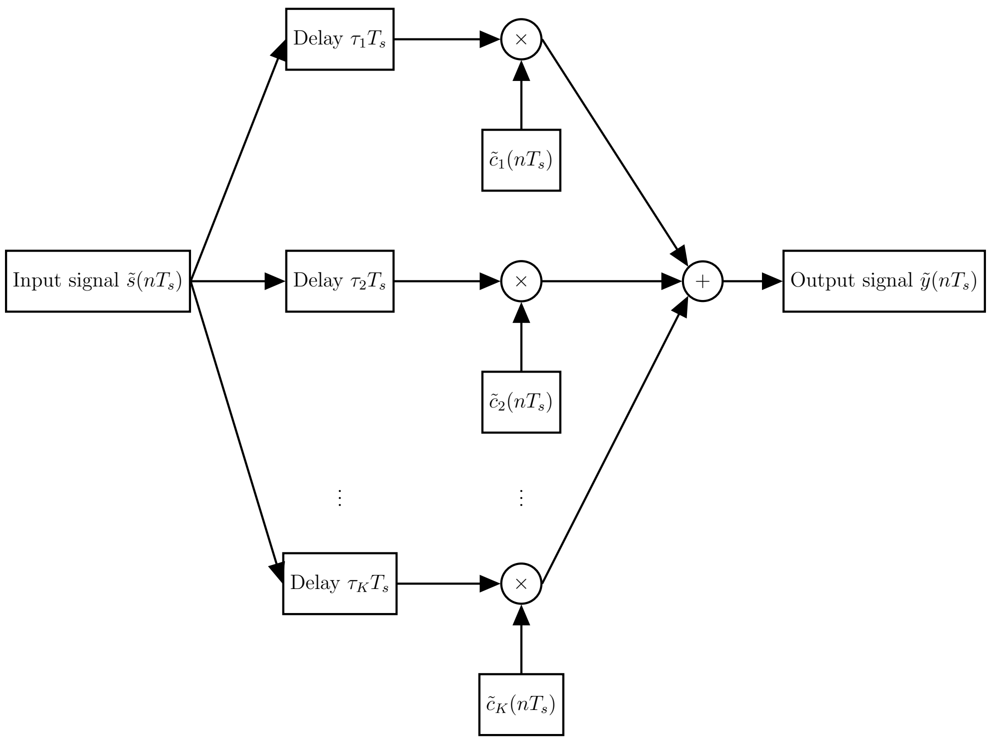

Figure 3: The principle of the tapped-delay-line channel model.

If the delay vector $\begin{bmatrix}50 & 250\end{bmatrix}$ [samples] is used to represent the delays, the output of the channel at time $300T_s$ is given as

$$\tilde{y}(300T_s) = \tilde{c}_1(300T_s)\tilde{s}\big((300-50)T_s\big) + \tilde{c}_2(300T_s)\tilde{s}\big((300-250)T_s\big) = \\ \tilde{c}_1(300T_s)\tilde{s}(250T_s) + \tilde{c}_2(300T_s)\tilde{s}(50T_s). \quad (19)$$

This means that τ in (18) is assumed to be equal to a sample n which is reasonable because if the delay is 50 [samples], what is received at time $300T_s$ was transmitted as sample $n = 250$ which is also seen in (19) as $\tilde{s}(250T_s)$. Motivated by this discussion, the output in the implementation is calculated as

$$\tilde{y}(nT_s) = \sum_{k=1}^{K} \tilde{c}_k(nT_s)\tilde{s}\big((n-\tau_k)T_s\big)$$

which is a modification of (18).

2.3.5 Power spectral density and autocorrelation

The implementation of multipath fading is done at baseband level. According to [9, page 6], the normalised Jakes Doppler spectrum at baseband level is

$$S(f) = \frac{1}{\pi f_d \sqrt{1-\left(\frac{f}{f_d}\right)^2}},\ |f| \le f_d \quad (20)$$

where Jakes Doppler spectrum is valid for a mobile receiver and implies that the propagation of the waves is horizontal, that the waves arrive with a uniformly distributed angle in the interval $[-\pi, \pi]$ and that an omnidirectional receive antenna is used [9, page 6]. In [3, page 3] the expression in (20) is multiplied with the variance σ^2 giving

$$S(f) = \frac{\sigma^2}{\pi f_d \sqrt{1-\left(\frac{f}{f_d}\right)^2}},\ |f| \le f_d \text{ (and 0 else)} \quad (21)$$

for Jakes power spectral density. However, as was also mentioned, the expression in (20) is normalised. The autocorrelation related to the expression in (20) is [9, page 6]

$$R(\tau) = J_0(2\pi f_d \tau) \quad (22)$$

where $J_0(...)$ is the Bessel function of the first kind having order zero. In [3, page 3] the expression for the autocorrelation is

$$\sigma^2 J_0(2\pi f_d \tau). \quad (23)$$

Usage of the variance σ^2 in the expressions for power spectral density and autocorrelation depends on if normalised expressions are wanted or not. It can be emphasised that the expressions for the power spectral density in (21) and for the autocorrelation in (23) are the same for both the real and imaginary part of $\mu(nT_s)$ in (15) [3, page 3]. In other words, (21) describes the power spectral density both for the real and imaginary part of $\mu(nT_s)$. The expression in (23) describes the autocorrelation both for the real and imaginary part of $\mu(nT_s)$.

2.3.6 Scaling of channel coefficients

The channel coefficients for the paths have to be scaled so that the total expected power is normalised to 1 and so that the individual paths can have different scalings which will create the effect that one path can be stronger than another path. The channel coefficient for path k at time nT_s is denoted as $c_k(nT_s)$, $k = 1, 2, ..., K, n = 0, 1, ..., N-1$ and $\mathbf{c}_k$ denotes a vector containing the channel coefficients for all samples $n \in [0, N-1]$ for path k. The expected power of path k is calculated as the expectation $E[|\mathbf{c}_k|^2]$. The simulated channel is a matrix if the number of paths $K > 1$ and it will have the following structure:

$$\begin{bmatrix} c_1(0) & c_1(1T_s) & \dots & c_1\big((N-1)T_s\big) \\ c_2(0) & c_2(1T_s) & \dots & c_2\big((N-1)T_s\big) \\ \vdots & \vdots & \ddots & \vdots \\ c_K(0) & c_K(1T_s) & \dots & c_K\big((N-1)T_s\big) \end{bmatrix}.$$

Since delays can be introduced between the paths, rows of zeros are to be inserted between the paths in the case when the delays are more than one sample. Then the simulated matrix can for example have the following structure:

$$\begin{bmatrix} c_1(0) & c_1(1T_s) & \dots & c_1\big((N-1)T_s\big) \\ 0 & 0 & \dots & 0 \\ 0 & 0 & \dots & 0 \\ c_2(0) & c_2(1T_s) & \dots & c_2\big((N-1)T_s\big) \\ c_3(0) & c_3(1T_s) & \dots & c_3\big((N-1)T_s\big) \\ \vdots & \vdots & \ddots & \vdots \\ c_K(0) & c_K(1T_s) & \dots & c_K\big((N-1)T_s\big) \end{bmatrix}.$$

In the implementation, the zeros are not inserted before scaling the channel coefficients. Instead it may be relevant to insert the zeros when calculating the output of the multipath fading channel so that the delays become correct.

In the implementation, zeros are used between the paths but only the non-zero rows affect the output of the multipath fading channel. However, the zeros can be useful when creating a figure of the channels' impulse response. Examples of the impulse responses of two channels are shown in Figure 16.

The process of scaling the channel coefficients is divided into three steps:

1. Normalise the expected power $E[|\mathbf{c}_k|^2]$ for each path k to be 1.
2. Scale the paths with scalings specified by the user.
3. Normalise the total expected power to be 1, i.e. so that $\sum_{k=1}^{K} E[|\mathbf{c}_k|^2] = 1$.

More details about each step are given in the following text.

Step 1 The expected power of the channel coefficients of a path k is calculated as the average $(1/N)\sum_{n=0}^{N-1} |c_k(nT_s)|^2$. The first step in the list is performed as the following scaling:

$$\hat{c}_k(nT_s) = \frac{\sqrt{N}}{\left|\left|\mathbf{c}_k\right|\right|} c_k(nT_s) \tag{24}$$

where $\left|\left|\mathbf{c}_k\right|\right|$ is a vector norm. The vector norm $\left|\left|\mathbf{c}_k\right|\right|$ of a complex vector $\mathbf{c}_k$ is calculated as $\sqrt{\sum_{n=0}^{N-1} c_k^2(nT_s)} = \sqrt{\sum_{n=0}^{N-1} |c_k(nT_s)|^2}$ [23] where $|...|$ is the complex modulus [20]. By performing the scaling in (24) the following holds:

$$\frac{1}{N}\sum_{n=0}^{N-1} |\hat{c}_k(nT_s)|^2 = \frac{1}{N}\sum_{n=0}^{N-1} \underbrace{\frac{N}{\left|\left|\mathbf{c}_k\right|\right|^2}}_{\text{Positive scalar}} |c_k(nT_s)|^2 =$$

$$\frac{1}{N}\frac{N}{\left|\left|\mathbf{c}_k\right|\right|^2}\sum_{n=0}^{N-1} |c_k(nT_s)|^2 = \frac{1}{\left|\left|\mathbf{c}_k\right|\right|^2}\left|\left|\mathbf{c}_k\right|\right|^2 = 1$$

meaning that the expected power of the channel coefficients of any path k will be 1. This means that the first step in the list is finished.

Step 2 The user can specify scalings for the individual paths. Since the channel coefficients will be normalised later in the third step in the list, these scalings only work in a relative sense. This means that if the user specifies $\begin{bmatrix}1 & 0.5\end{bmatrix}$ as scalings for the paths it will not mean that the expected power for the paths will be 1 and 0.5 but it will mean that the first path is twice as strong as the second path. The channel coefficients $\hat{c}_1(nT_s)$ and $\hat{c}_2(nT_s)$ will be multiplied with $\sqrt{1}$ and $\sqrt{0.5}$ respectively. This means that if $\hat{\mathbf{c}}_k$, $k = 1, 2$ are defined to denote vectors containing the channel coefficients for the two paths at all samples $n \in [0, N-1]$ the expected power for these two paths becomes

$$\begin{cases} E[|\sqrt{1}\hat{\mathbf{c}}_1|^2] = \frac{1}{N}\sum_{n=0}^{N-1} |\sqrt{1}\hat{c}_1(nT_s)|^2 = 1 \,(\text{Step 1}) \\ E[|\sqrt{0.5}\hat{\mathbf{c}}_2|^2] = \frac{1}{N}\sum_{n=0}^{N-1} |\sqrt{0.5}\hat{c}_2(nT_s)|^2 = 0.5 \underbrace{\frac{1}{N}\sum_{n=0}^{N-1} |\hat{c}_2(nT_s)|^2}_{=1\,(\text{Step 1})} = 0.5 \end{cases}.$$

Step 3 If the expected power is calculated for all paths $k = 1, 2, ..., K$ the following vector is obtained:

$$\mathbf{p} = \frac{1}{N}\begin{bmatrix} \sum_{n=0}^{N-1} |\hat{c}_1(nT_s)|^2 \\ \sum_{n=0}^{N-1} |\hat{c}_2(nT_s)|^2 \\ \vdots \\ \sum_{n=0}^{N-1} |\hat{c}_K(nT_s)|^2 \end{bmatrix}.$$

Then the total expected power of the channel coefficients of all paths is given by the summation of the elements in the vector $\mathbf{p}$, i.e. by the summation $\sum_{k=1}^{K} \mathbf{p}(k) = \sum_{k=1}^{K}(1/N)\sum_{n=0}^{N-1} |\hat{c}_k(nT_s)|^2$, where $\mathbf{p}(k)$ denotes element k in the vector $\mathbf{p}$. According to [9, page 9 and 10] a Rayleigh channel created in MATLAB by `rayleighchan` has a property `NormalizePathGains` which would imply that this summation would be equal to 1. This means that there exists some scaling ϵ such that

$$\epsilon \sum_{k=1}^{K} \mathbf{p}(k) = 1. \tag{25}$$

This scaling can be found according to

$$\sum_{k=1}^{K} \frac{1}{N} \sum_{n=0}^{N-1} |\hat{c}_k(nT_s)|^2 = \frac{1}{\epsilon} \rightarrow \epsilon = \frac{1}{\sum_{k=1}^{K} \frac{1}{N}\sum_{n=0}^{N-1} |\hat{c}_k(nT_s)|^2}.$$

Then the channel coefficients are scaled according to $\sqrt{\epsilon}\hat{c}_k(nT_s)$ giving the new channel coefficients $\tilde{c}_k(nT_s)$ expressed as

$$\tilde{c}_k(nT_s) = \frac{\hat{c}_k(nT_s)}{\sqrt{\sum_{k=1}^{K} \frac{1}{N}\sum_{n=0}^{N-1} |\hat{c}_k(nT_s)|^2}}.$$

This means that the expected power of the new channel coefficients $\tilde{c}_k(nT_s)$ at path k will be

$$\frac{1}{N}\sum_{n=0}^{N-1}|\tilde{c}_k(nT_s)|^2 = \frac{1}{N}\sum_{n=0}^{N-1}\left|\frac{\hat{c}_k(nT_s)}{\sqrt{\sum_{k=1}^{K}\frac{1}{N}\sum_{n=0}^{N-1}|\hat{c}_k(nT_s)|^2}}\right|^2 =$$

$$\underbrace{\frac{N}{\sum_{k=1}^{K}\sum_{n=0}^{N-1}|\hat{c}_k(nT_s)|^2}}_{\text{Positive scalar}}\frac{1}{N}\sum_{n=0}^{N-1}|\hat{c}_k(nT_s)|^2 =$$

$$\frac{1}{\sum_{k=1}^{K}\sum_{n=0}^{N-1}|\hat{c}_k(nT_s)|^2}\sum_{n=0}^{N-1}|\hat{c}_k(nT_s)|^2. \quad (26)$$

In the example in the second step, $E[|\hat{\mathbf{c}}_1|^2] = 1$ and $E[|\hat{\mathbf{c}}_2|^2] = 0.5$ and the expected power of these paths after Step 3 can be calculated. This is done by using this information about the expected power of the two paths after Step 2 and (26), which gives

$$\begin{cases} \frac{1}{N}\sum_{n=0}^{N-1}|\tilde{c}_1(nT_s)|^2 = \frac{1}{1+0.5}1 = \frac{2}{3} \\ \frac{1}{N}\sum_{n=0}^{N-1}|\tilde{c}_2(nT_s)|^2 = \frac{1}{1+0.5}0.5 = \frac{1}{3} \end{cases}. \quad (27)$$

It can be seen in (27) that $\sum_{k=1}^{2}(1/N)\sum_{n=0}^{N-1}|\tilde{c}_k(nT_s)|^2 = 1$ (property of third step) and that the expected power of the channel coefficients of the first path is twice as large as for the second path (property of second step). As was shown by the example the total expected power of the channel coefficients of all paths is always 1 which is also reasonable because it means that no power is gained or lost because of multipath fading. If it would be 5 for example, the channel would imply an amplification of the input signal that is passed through the channel which is not realistic because multipath fading does not amplify (or attenuate) to such large extent.

It should be mentioned that the expected signal power is not exactly the same before and after the multipath fading channel but it does not vary very much. A power ratio which compares the expected power before and after multipath fading is calculated as

$$\text{Power ratio} = \frac{\frac{1}{N}\sum_{n=0}^{N-1}|s(nT_s)|^2}{\frac{1}{N}\sum_{n=0}^{N-1}|\tilde{s}(nT_s)|^2}$$

where $s(nT_s)$ is the signal before the multipath fading channel and $\tilde{s}(nT_s)$ is the signal after the multipath fading channel. It has been seen that

Power ratio in the case of Rayleigh fading typically is in the interval $[0.97, 1.03]$, i.e. the expected signal power almost does not change because of the multi-path fading. For Rician fading it has been seen that Power ratio typically is in the interval $[0.94, 1.06]$ so it varies more for Rician fading than for Rayleigh fading. Even if the ratio varies more for Rician fading, the ratio is relatively close to 1.00.

2.3.7 Rician fading

In the case of Rician fading, the expression in (13) describing the received electric field will be modified to contain also a line-of-sight component which will be stronger than the other components [9, page 2]. The modified expression can be written as [9, page 2]

$$E_{\text{received}}(nT_s) = A\cos(2\pi f_c nT_s + \theta_0) + \sum_{l=1}^{L} \bar{E}_l C_l \cos\big(2\pi f_c nT_s + \theta_l(nT_s)\big)$$

where A is a constant amplitude. Since the channel coefficients in the case of Rayleigh fading are generated by (16) it is actually (16) that will be modified. In [4, page 799] the following expression is used:

$$x(nT_s) = \sqrt{\frac{K\Omega}{K+1}} e^{j\left(2\pi f_d \cos(\theta_0) nT_s + \phi_0\right)} + \sqrt{\frac{\Omega}{K+1}} h(nT_s) \tag{28}$$

where $x(nT_s)$ is the received signal at baseband level, K denotes the Ricean factor, θ_0 is the angle with which the line-of-sight component is received, ϕ_0 is the phase of that component and $h(nT_s)$ describes the components that are not line-of-sight. The term $h(nT_s)$ is a complex Gaussian process [4, page 799] so $h(nT_s)$ represents reflections due to local scattering meaning that the previously found Gaussian process can be used as $h(nT_s)$. That the previously found Gaussian process that was obtained by summing many sinusoids to describe local scattering can be used, is also supported by the fact that $h(nT_s)$ is obtained by the summation of many multipath components [4, page 799]. So $h(nT_s)$ is given by (15) and (16). In (28), f_d denotes maximum Doppler frequency [4, page 799]. It is assumed that $\theta_0 = \phi_0 = 0$. If $c_k(nT_s)$ replaces $h(nT_s)$ while $\dot{c}_k(nT_s)$ replaces $x(nT_s)$ in (28), the expression can be rewritten. The following expression for the Rician multipath fading channel coefficients can then be obtained:

$$\dot{c}_k(nT_s) = \frac{1}{\sqrt{K+1}} \sqrt{\Omega_k} c_k(nT_s) + \sqrt{\frac{K}{K+1}} \sqrt{\Omega_k} \big(\cos(2\pi f_d nT_s) + j\sin(2\pi f_d nT_s)\big) \tag{29}$$

where Ω_k is the expected power of path k [9, page 9]. Combining this with Step 1 and Step 2 in section 2.3.6 means that first Step 1 is to be applied to $c_k(nT_s)$. Then Step 1 will be applied to $\dot{c}_k(nT_s)$. Step 1 does not have to be applied to $\cos(2\pi f_d nT_s) + j\sin(2\pi f_d nT_s) = e^{j2\pi f_d nT_s}$ because $(1/N)\sum_{n=0}^{N-1} |e^{j2\pi f_d nT_s}|^2 = 1$. The multiplication with $\sqrt{\Omega_k}$ is exactly what is done in Step 2 since this multiplication represents how strong path k should be. This means that the multiplication with $\sqrt{\Omega_k}$ is done in Step 2 and not as in (29). If there are more paths than the Rician fading path, Step 1 and Step 2 also have to be applied to these paths before Step 3 can be applied to all paths.

The probability density function of a channel envelope $|c|$ having Rician fading (i.e. following a Rician probability distribution) can be written as [9, page 2]

$$p_C(|c|) = \frac{2|c|}{\Omega} e^{-\frac{A^2+|c|^2}{\Omega}} I_0\left(\frac{2A|c|}{\Omega}\right), |c| \geq 0 \tag{30}$$

where $I_0(...)$ represents the modified Bessel function with order 0 and A is the amplitude of the line-of-sight component [9, page 2]. The ratio A^2/Ω is called the Rician K-factor [9, page 2]. The Rician K-factor defines how much stronger the line-of-sight component is than the scattered components [12]. This can be seen by using (29) according to

$$\frac{\text{Expected power, line-of-sight component}}{\text{Expected power, scattered components}} = \frac{\left|\sqrt{\frac{K}{K+1}}\sqrt{\Omega_k}\right|^2}{\left|\frac{1}{\sqrt{K+1}}\sqrt{\Omega_k}\right|^2} = K$$

where it was used that after Step 1, $E[|\mathbf{c}_k|^2] = 1 = (1/N)\sum_{n=0}^{N-1} |e^{j2\pi f_d nT_s}|^2$. Typical values in a linear scale for the Rician K-factor is between 1 and 10 [12]. In MATLAB the command `ricianDistribution = fitdist(c,'Rician')` would return the parameters of the Rician distribution for a vector `c` by using maximum likelihood estimation [13]. These parameters would be called `s` and `sigma` [14]. In [15], the definition of the Rician distribution has the form

$$I_o\left(\frac{xs}{\sigma^2}\right)\frac{x}{\sigma^2}e^{-\frac{x^2+s^2}{2\sigma^2}}, x > 0 \tag{31}$$

where I_0 represents the modified Bessel function with order zero of the first kind and x is the data. Some comparison of the expression in (30) and the expression in (31) gives that the following holds:

$$\begin{cases} \Omega = 2\sigma^2 = 2\texttt{sigma}^2 \\ A = s = \texttt{s} \\ |c| = x \end{cases} .$$

Since $K = A^2/\Omega$, the Rician K-factor can be calculated as $\texttt{s}^2/(2\texttt{sigma}^2)$.

3 Description of the system

This section presents a description of how the implemented simulator tool works. To summarise, the transmission is done in the computer by passing a signal through a simulated communication channel in the computer. Then the result of that simulated transmission is passed to a car radio by an instrument via a cable. The simulator tool contains four main features which are:

- Input and output of files
- FM radio signal generation
- Multipath fading channel (Rayleigh fading and Rician fading)
- Path loss and shadowing

The simulator tool is divided into four tabs and these tabs contain options for the items in the list in this section. This section will describe the four tabs more and contain figures of the tabs. The figures of the tabs contain the default settings of the simulator tool. When starting the simulator tool, these default settings are shown and the user has the possibility to do changes of the settings.

3.1 Overview of the simulator tool

Figure 4 shows an overview of the implementation of the simulator tool. The implementation of creation of FM signal, multipath fading channel, path loss and shadowing is based on the methods described in section 2. The user can create an FM signal having a single-frequency tone or contents from a loaded audio file as information. The simulator tool supports audio files in terms of .mp3 files. Instead of creating an FM signal, the user can load a file containing an FM or DAB broadcast and use in the simulator tool. When a signal has been created or loaded, the signal will pass a multipath fading channel. After that, path loss and shadowing effects are potentially added to the signal. The signal can be used with an instrument called Universal Receiver Tester (URT) which can pass the signal to a car radio.

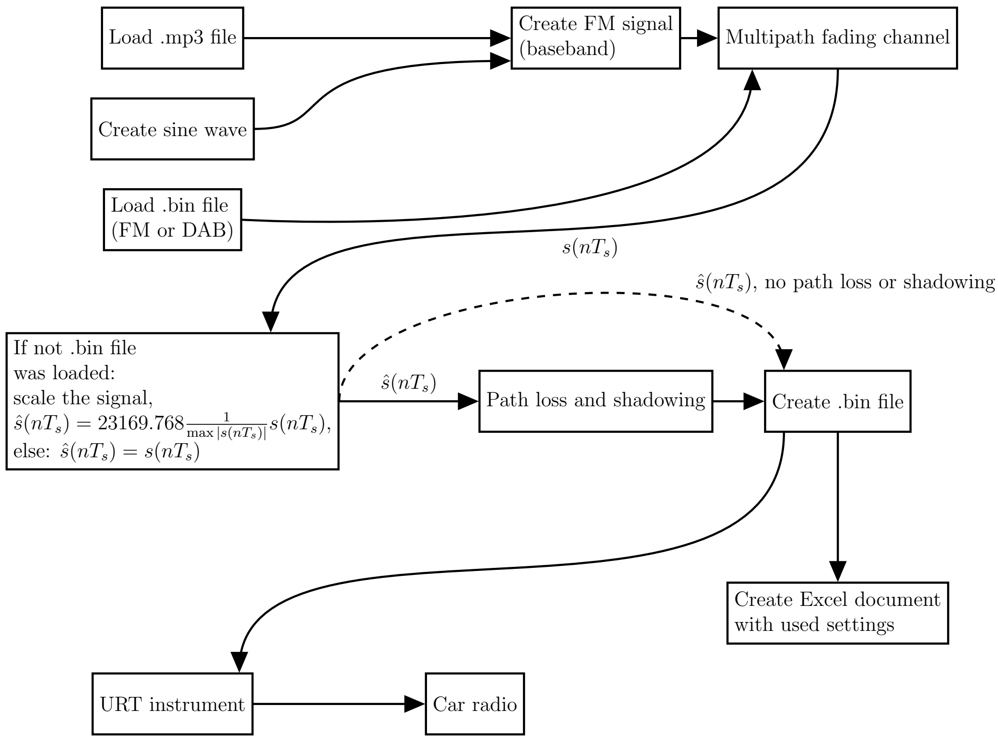

Figure 4: Overview of the simulator tool.

The scaling $23169.768\big(1/(\max|s(nT_s)|)\big)$ in Figure 4 has shown to be good with a gain setting of the URT instrument of $1 \cdot 10^{-4}$ (mentioned in section 3.2.1) in the sense that it gives a power level slightly below 0 [dBm] if path loss and shadowing is not used. The signal values are written to a file in an `int16` format and this format in MATLAB means that values in the interval $[-32768, 32767]$ are covered [18]. So the signal values have to be in this interval and if they are not, they will be clipped to -32768 or 32767 depending on sign of the signal values. The scaling in the simulator tool implies that the signal values can at most have an absolute value equal to 23169.768 at that step after the scaling has been performed. Scaling by the number $23169.768\big(1/(\max|s(nT_s)|)\big)$ is motivated only by the fact that it seems to work well with the mentioned gain setting. For a lower gain setting, it is likely that the number could be increased and replaced by for example $25000.000\big(1/(\max|s(nT_s)|)\big)$. When looking at the power levels after multipath fading, path loss and shadowing, it has been seen that the power levels in for example Figure 21a are approximately the same as in the URT instrument. There may be some differences and it is somewhat difficult to track the power levels since they change quickly but the differences are not very large and it should be good enough. However, precision on the order of a 1 [dBm] scale can not be guaranteed. This is due to the gain setting of the URT instrument in combination with the described scaling. More work can be done regarding this. One solution could be to scale the signal values so that they are in the interval $[-32768, 32767]$ and then find the gain setting of the URT instrument that gives a level of 0 [dBm], assuming that such setting exists.

The scaling in Figure 4 is not performed if a .bin file is loaded into the simulator tool. If such a file is loaded into the simulator tool, the gain setting will be the same as it was for that file. Then the scaling may be inaccurate so therefore it is not used in that case.

3.2 Input and output of files

The simulator tool has several capabilities for input and output of files. The most important capability is the functionality for the output of a .bin file which can be used by the URT instrument for passing the content of that file to a car radio. The user can load audio contents from an .mp3 file and create an FM radio signal with a stereo audio signal as information. The stereo audio signal is based on the contents of the .mp3 file. The user can also load .bin files which can for example contain FM or DAB radio recordings. Then channel effects can be added to these recordings in the tool and a modified .bin file is the output which can be used with a car radio. An Excel document with all the used settings is automatically created. This section presents how the functionalities for input and output of files work. Figure 5 shows the tab for settings related to input and output of files in the simulator tool.

3.2.1 URT file

The URT instrument was used for passing the signals to a radio. The information of e.g. which carrier frequency and sampling frequency to use with the instrument was decided by header information that is included in the file that was created in the computer when the output of the communication channel (in the computer) was saved to a file. This means that the selected carrier frequency and sampling frequency (in the GUI) is written as header information being positioned in the beginning of the data of the file that is created.

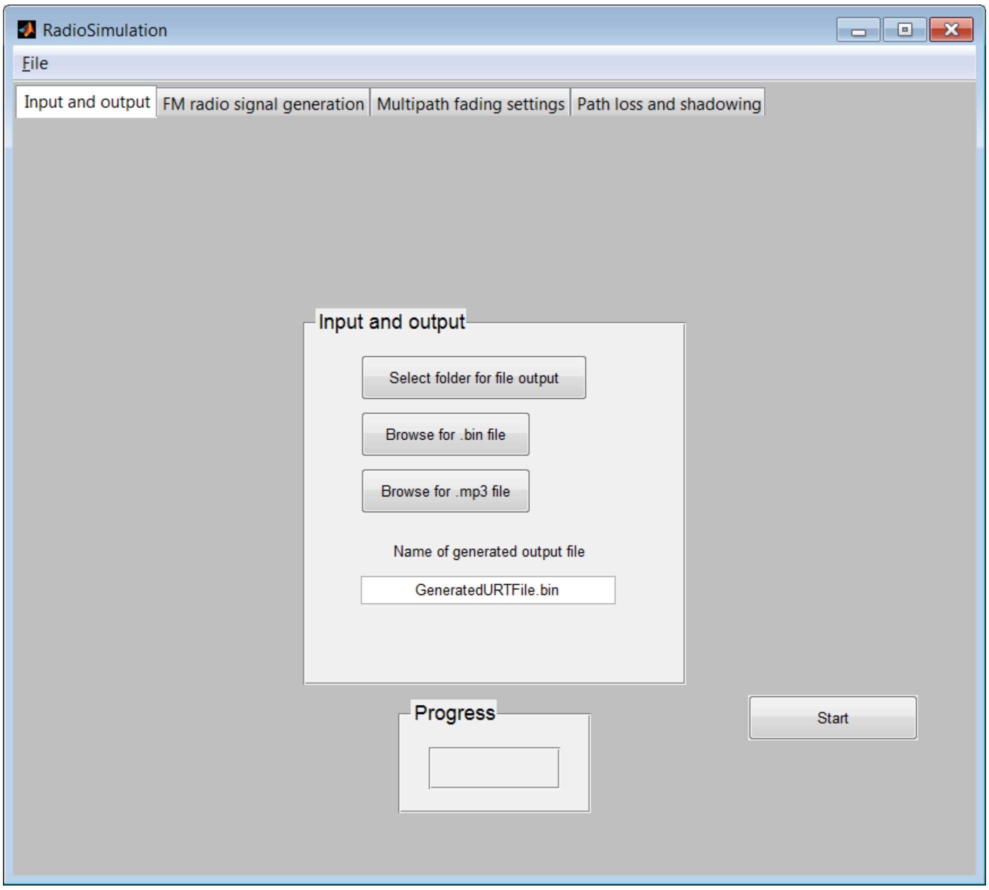

Figure 5: Tab for settings related to input and output of files.

The file that is created is a .bin file and this file can be used by the URT instrument. The data in the .bin file should be a baseband signal. The samples having an odd index correspond to the in-phase part of the created signal and the samples having an even index correspond to the quadrature-phase part of the created signal. This means that the in-phase signal values are positioned at indices $1, 3, ..., N_{\text{URT}} - 1$ where $N_{\text{URT}} = 2N$ is the number of samples of the created .bin file. The quadrature-phase signal values are positioned at indices $2, 4, ..., N_{\text{URT}}$ and index 1 is the first index. The original vector of N complex numbers becomes a vector of $2N = N_{\text{URT}}$ real numbers by positioning the signal values in this way. The following information has to be included in the header information and the used values are presented within parentheses:

- 0 (0)

- Version (1), related to software version
- Sampling frequency in Hz (selected in the GUI)
- Carrier frequency in Hz (selected in the GUI)
- Reference level in dBm (0)
- Power in dBm (0)
- Start time in seconds (0)
- Gain ($1 \cdot 10^{-4}$)
- Offset (0)
- Little endian (1)
- External gain loss (0), related to pre-amplification of the signal

Many of these values are default values that are used in a MATLAB example given in the MATLAB RF Record and Playback Toolbox which was given to Averna's RF Signal Record and Playback System (the URT is a product of Averna). According to that example, the number 0 included first in the header information is a preamble. If the header information is not correctly created, the URT can not use the created .bin file. Therefore it is important to have the header information in the correct format. If the option to load a .bin file into the simulator tool is used, the header information is the same as it was for that .bin file, i.e. for example power and carrier frequency is the same as it was for the loaded file. More information about the header information of a URT file is given in section A.1.

3.2.2 Audio file (.mp3)

The .mp3 file is loaded into the simulator tool by the MATLAB function `audioread` which returns data from the .mp3 file in the interval $[-1.0, 1.0]$ and also the sampling frequency for that data [16]. This sampling frequency could be for example 44100 [Hz] but the sampling frequency of the FM radio signal that will be created for example 1 [MHz]. Therefore, the sampling frequency of the loaded audio file has to be changed to match this higher sampling frequency. This is done by using the MATLAB function `resample` which for the given example would resample the signal by the factor $(1 \cdot 10^6\,[\text{Hz}])/(44100\,[\text{Hz}])$ [19]. For this example, the length of the audio signal after resampling would be: $\text{Round}\big(\text{length before resampling} \cdot (1 \cdot$

10^6 [Hz])/(44100 [Hz])). This means that the length of the audio signal can become very long and the amount of data may be unsuitable for the computer. Therefore, a limit of $1.5 \cdot 10^7$ [samples] after the resampling is used in the tool meaning that data is possibly removed from the original input audio signal until the length is such that the following holds:

$$\text{Round}\big(\text{length before resampling}\cdot \\ (\text{Sampling frequency})/(\text{Sampling frequency, audio file})\big) \leq \\ 1.5 \cdot 10^7 \,[\text{samples}].$$

A loop is used and in each iteration, $1 \cdot 10^4$ [samples] are removed from the end of the loaded audio signal until this criterion is fulfilled.

When the audio signal has an appropriate number of samples, the stereo audio signal is created according to (5). Then the in-phase and quadrature-phase components of the FM radio signal are created according to (4). The integral is solved numerically and it is solved once. Then that numerical solution is used for both components. Before the stereo audio signal is created, the contents of the audio file is scaled so that its maximum absolute value is 1 according to the discussion in section 2.1.1 related to frequency deviation and modulation levels.

3.2.3 Excel document

After each simulation, an Excel document is generated automatically. This Excel document contains information about all the settings that were used in the simulation. The name of the document contains information about the date and time when it was created. An example of such Excel document is included in section A.2.

3.3 FM radio signal generation

The functionality for FM radio signal generation enables creation of an FM radio signal and thereby full control of the transmission. Full control implies that the signal is a perfect FM radio signal and it has for example not been attenuated which could be the case if using recorded FM radio signals. Together with usage of the URT instrument for passing the FM radio signal to a radio, this means that the user can technically create an own radio station broadcast file to be passed by cable to a car radio.

When a single-frequency tone is used as information, the created audio signal is a mono signal and there is no pilot tone at 19 [kHz]. This means that the mono signal, which is a sinusoid, gets at most 100 [%] of the frequency deviation. The single-frequency tone used in the simulator tool is implemented as the sinusoid

$$m(nT_s) = A_m \cos(2\pi f_m nT_s) \tag{32}$$

where the amplitude A_m and the frequency f_m can be selected as settings in the simulator tool. The information $m(nT_s)$ can also be said to be an information signal and the difference between the FM signal and the information signal is clear.

When an audio file is loaded into the simulator tool, the audio signal that is created based on the contents of the file, is a stereo signal and there will be a pilot tone at 19 [kHz]. If the user wants to create a mono signal which has a pilot tone, an audio file having the same contents in both audio channels can be loaded into the simulator tool. The simulator tool creates the signal as if it would be a stereo signal, but since left and right audio channels are the same, there will be no stereo contents of the created signal. So a mono audio signal is created and it gets at most 90 [%] of the frequency deviation and the pilot tone has at most 10 [%] of the frequency deviation.

The settings for the signal that is to be transmitted can be adjusted in the tab “FM radio signal generation”. For each simulation the following settings can be done for the FM signal generation:

- If a sinusoid is to be used as information signal
- Carrier frequency
- Message frequency (only applicable if a sinusoid is used as information signal)
- Sampling frequency
- Frequency deviation
- Length of the signal (samples)
- Amplitude of the signal (only applicable if a sinusoid is used as information signal)

When loading a .mp3 file into the simulator tool, the settings for carrier frequency, sampling frequency and frequency deviation can be adjusted in this tab. If the alternative to use a sinusoid as information signal is not selected, a URT file (.bin file) or audio file (.mp3 file) has to be loaded into the simulator tool. The user does not have to press a button which says that e.g. an audio file is to be used. Instead the user has to load an audio file and make sure that "Use sinusoid as information" is not selected. The last setting in the list, i.e. the amplitude of the signal, will set a value of the constant A_m mentioned for example in (32). Figure 6 shows the tab for settings related to the generation of an FM radio signal in the simulator tool.

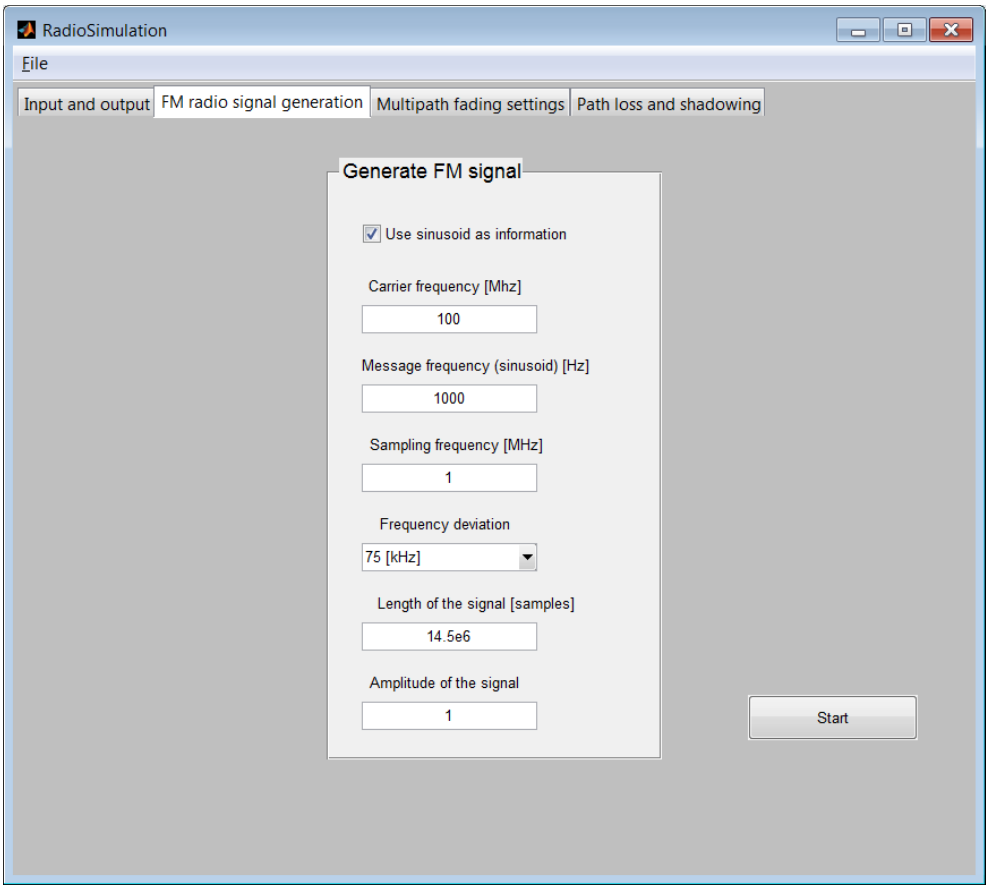

Figure 6: Tab for settings related to FM radio signal generation.

3.4 Communication channel

The communication channel was created and used in the computer and is where the thesis project has its emphasis. In particular multipath fading effects are central. Therefore, the user of the simulator tool can adjust many settings regarding multipath fading. Many settings can be adjusted also for path loss and shadowing. This gives the possibility for the user to have control of these effects and it also enables the possibility to create many different cases of multipath fading, path loss and shadowing that can be tested with a car radio.

3.4.1 Multipath fading

For each simulation the following settings can be done for the multipath fading:

- Rayleigh fading (no line-of-sight component) or Rician fading (one line-of-sight component)
- Number of paths
- Velocity of the car
- Delays for each path (in number of samples)
- Number of sinusoids that will be used to create the fading channel coefficients
- Rician K-factor
- Number of samples of the channel
- Scalings for each path, i.e. how strong the paths should be relative each other

A maximum likelihood estimate of the Rician K-factor is returned so that the user can see if this estimate is close to the Rician K-factor that was defined as user input. This estimate of the Rician K-factor is calculated according to the method described in section 2.3.7. When Rayleigh fading is selected, all paths have Rayleigh fading. When Rician fading is selected, the first path has Rician fading and if more than one paths are selected, the other paths have Rayleigh fading. This is reasonable according to Figure 2 where a signal at the path with line-of-sight communication will arrive first. This path will have Rician fading and the other paths will have Rayleigh fading because there is no line-of-sight communcation for these paths. Figure 7 shows the tab for settings related to multipath fading in the simulator tool.

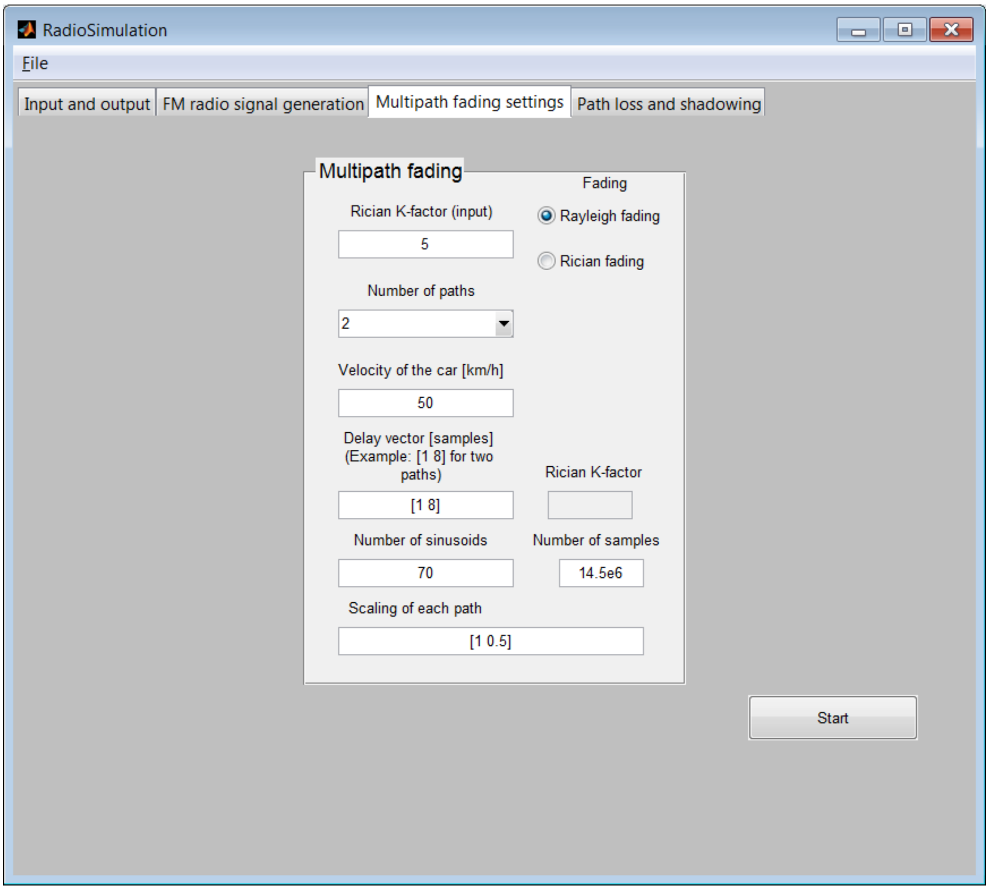

Figure 7: Tab for settings related to multipath fading.

3.4.2 Path loss and shadowing

For each simulation the following settings can be done for path loss and shadowing:

- If path loss and shadowing is to be used
- Transmit power of radio station
- Start distance from radio station (transmitter)
- Decorrelation distance
- Standard deviation log-normal distribution
- Reference distance

- Path-loss exponent (gamma)

The velocity has impact on how quickly the shadowing decorrelates since it decides how quickly the decorrelation distance can be reached. The velocity also has an impact on the path loss since the path loss will increase as the distance between the car and the transmitter increases. The velocity is the same as the velocity that was selected for the multipath fading. Figure 8 shows the tab for settings related to path loss and shadowing in the simulator tool.

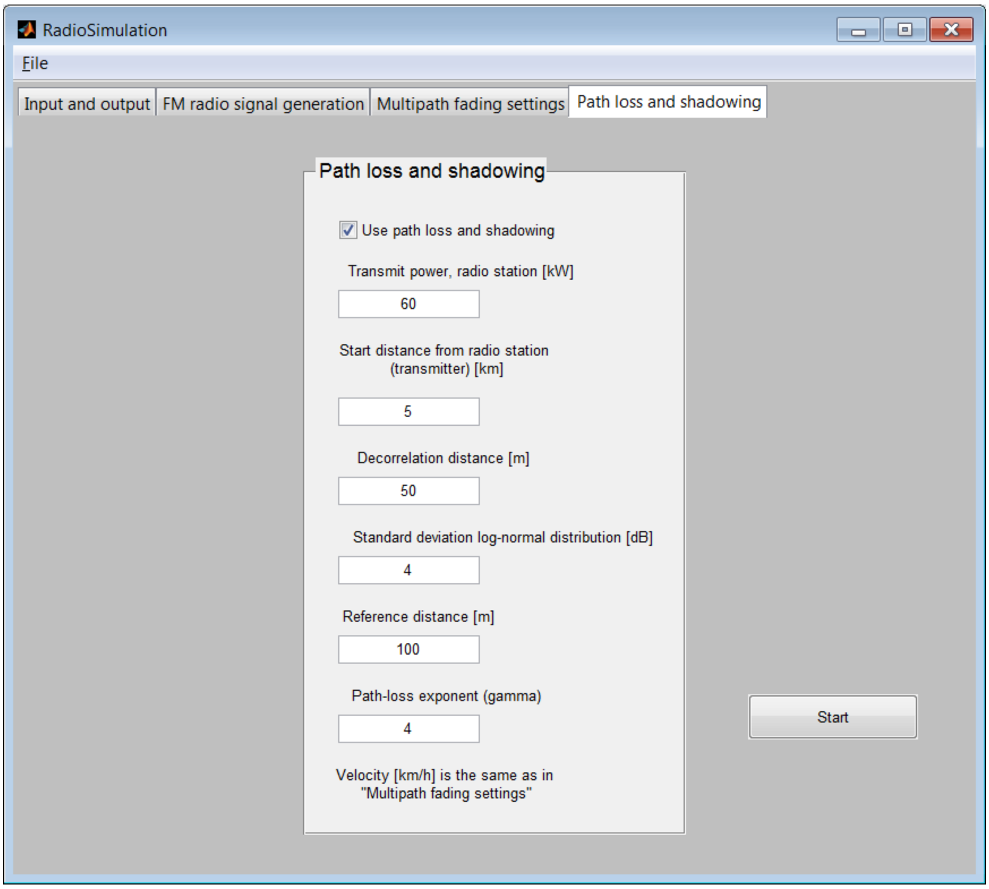

Figure 8: Tab for settings related to path loss and shadowing.

3.5 Receiver

The receiver was a Volvo car radio with possibilities to receive both analog (AM and FM) and digital (DAB) radio signals. A car was not needed when passing the signal to the radio and the radio was connected to the URT instrument by a cable. The radio was connected to loudspeakers so that it was possible to hear the output of the radio. The radio does not have to be a Volvo car radio and for example radios that are in an early stage of a development process can be tested if the radios are compatible with the URT instrument. In this way, radios by several suppliers can be tested early with regards to multipath fading, path loss and shadowing. A ROHDE&SCHWARZ UPV Audio Analyzer has been connected after the radio and this is a possibility to do measurements. This possibility can be studied somewhat more to find out what parameters are appropriate to measure.

4 Results

This section presents results from the simulator tool in terms of figures, which are verified by comparison to theory. The section has a focus on verification of the used methods and therefore the section is a motivation to why the simulator tool is reliable. The results are divided into three sections that correspond to three tabs in the simulator tool, i.e. sections about FM radio signal generation, multipath fading and path loss and shadowing. Most of the figures that follow, were given by a simulation by using the simulator tool. For this simulation, the default settings were used. This implies usage of multipath fading (Rayleigh fading), path loss and shadowing and an FM radio signal was created from the very beginning with a sinusoid as information signal. The used settings can be found in section A.2 where the Excel document from the simulation has been included. Some figures from a Rician fading simulation are included as well and comparisons between Rayleigh fading and Rician fading are done. For the Rician fading simulation, a Rician K-factor of 5 was used.

4.1 FM radio signal generation

Figure 9 shows excerpts of the in-phase and quadrature-phase components of the FM signal before any effects have been applied and an excerpt of the information. The excerpts were created by only using short time intervals of the in-phase and quadrature-phase components and information. Since default settings were used, the frequency of the sinusoid was 1000 [Hz]. The corresponding period time of $1 \cdot 10^{-3}$ [s] can be seen in the figure for the information and for the in-phase and quadrature-phase components of the FM signal.

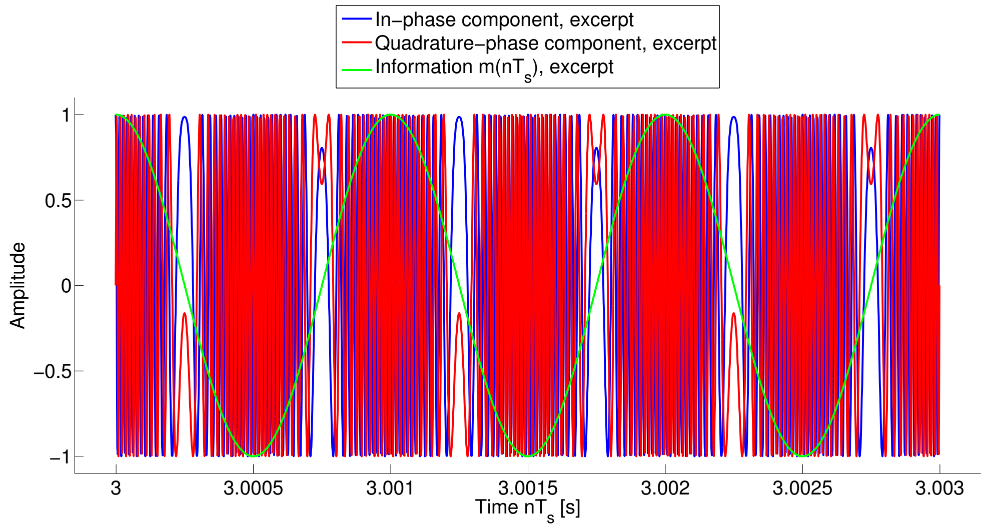

Figure 9: Excerpts of the in-phase and quadrature-phase components of the FM signal before any effects have been applied and an excerpt of the information.

4.2 Multipath fading

Figure 10 shows the probability density functions (PDFs) of the in-phase and quadrature-phase components of the generated channel coefficients for the first and second path of a Rayleigh fading channel simulation. For each such PDF, a normal PDF is also shown. Both paths were Rayleigh fading paths. The real part of the channel coefficients represents the in-phase components and the PDFs for these components are in the figures to the left. The imaginary part of the channel coefficients represents the quadrature-phase components and the PDFs for these components are in the figures to the right. All the PDFs in the report were calculated as histograms, which were normalised such that they integrate to 1. The histograms were always calculated at 250 intervals.

As can be seen in section A.2, the first path had the scaling 1 and the second path had the scaling 0.5 meaning that the first path is twice as strong as the second path. The delays for the paths were 1 [sample] and 8 [samples]. The scalings and the delays can not be seen in Figure 10. The scalings can not be seen in the figure since the scalings have not been applied to the channel coefficients at this stage. However, it can be relevant to mention the scalings and the delays for coming figures.

Figure 11 shows the PDF estimated from the channel coefficients for Rayleigh fading and a Rayleigh PDF. The figure to the left is for the first

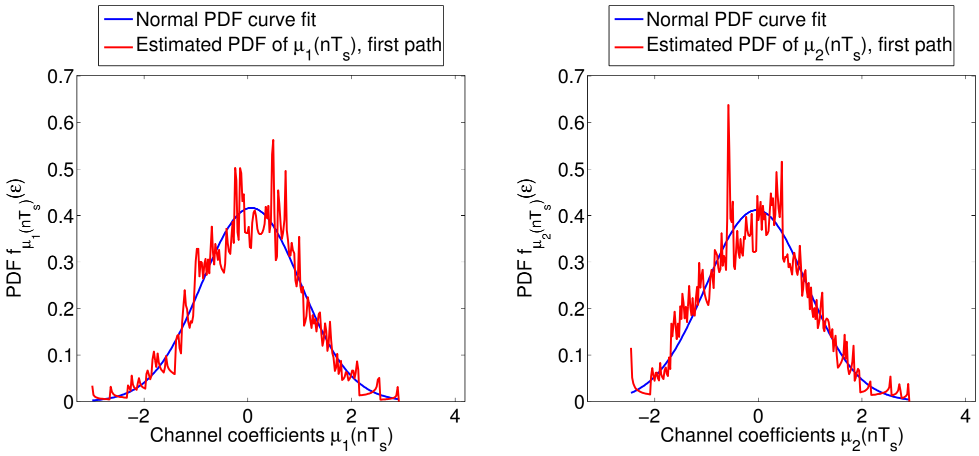

(a) First path.

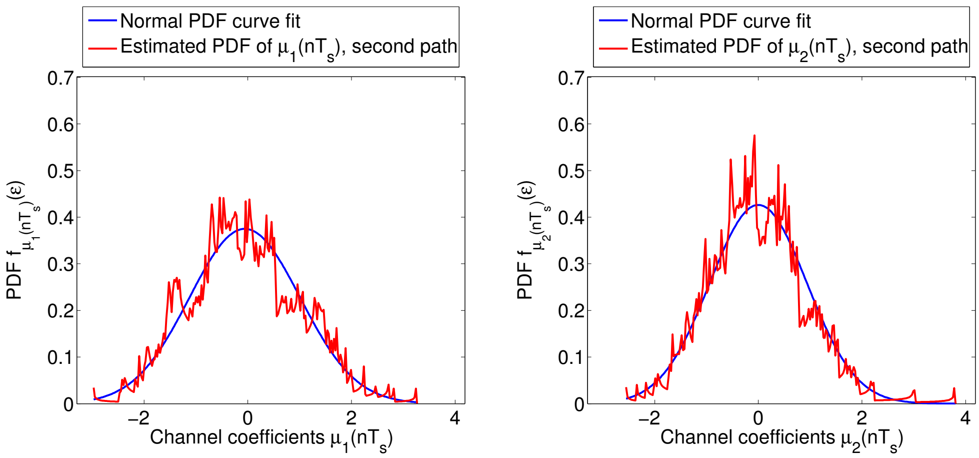

(b) Second path.

Figure 10: PDFs of in-phase and quadrature-phase components of the generated channel coefficients for the first (a) and second (b) path. For each such PDF, a normal PDF is also shown.

path and the figure to the right is for the second path. It can be seen that the first path in general is stronger than the second path which is expected due to the scalings previously described.

Figure 12 shows the PDF estimated from the channel coefficients for Rician fading and a Rician PDF. In the figure, $|c_1(nT_s)|$ represents the absolute value of the channel coefficients of the first path. This path is a Rician fading path. The maximum likelihood estimate of the Rician K-factor is shown in the title of the figure.

Figure 13 shows the envelope $20\log_{10}|c(nT_s)|$ for Rayleigh fading and Ri-

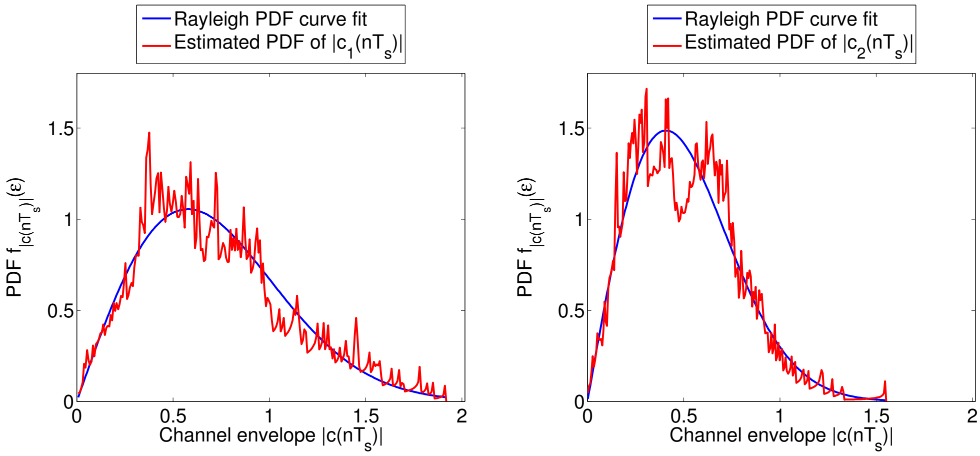

Figure 11: Estimated PDF and Rayleigh PDF. The figure to the left is for the first path and the figure to the right is for the second path.

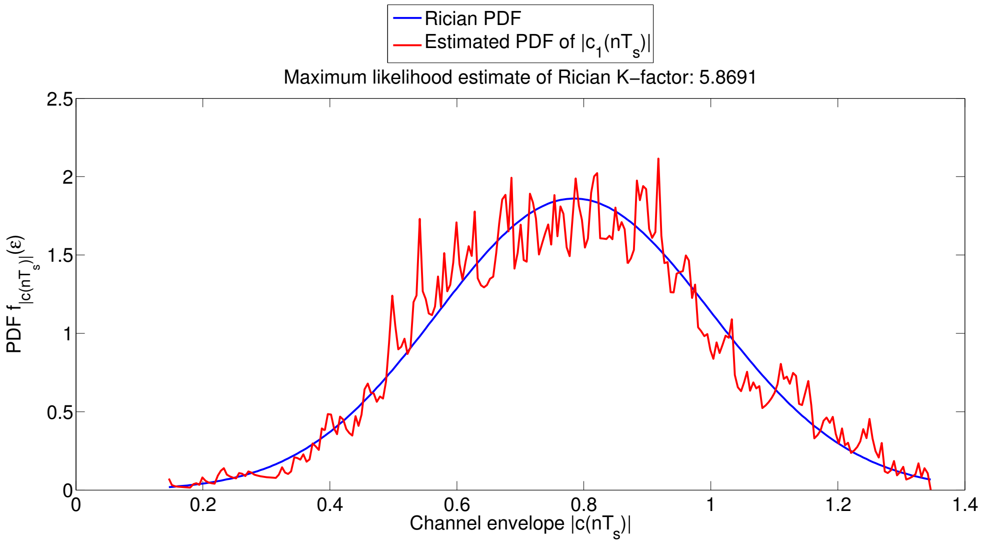

Figure 12: Estimated PDF, Rician PDF and maximum likelihood estimate of Rician K-factor.

cian fading, where $c(nT_s)$ are the channel coefficients of the first path. Figure 13a shows the envelope of the first path of the channel when Rayleigh fading was used for both paths. Figure 13b shows the envelope of a Rician fading path. Two paths were created for this simulation and for the first path Rician fading was used which means that in Figure 13b the first path of the channel is shown. It can be seen that at some times, the channel drops quickly and much in power both in the case of Rayleigh and Rician fading. This is a result of the multipath fading. It can be seen that compared to the Rayleigh fading channel envelope in Figure 13a, the channel envelope does not drop as much in power for Rician fading as it does for Rayleigh fading. This is expected because the line-of-sight property of Rician fading is expected to give a channel which does not attenuate a signal as much as a Rayleigh fading channel would do.

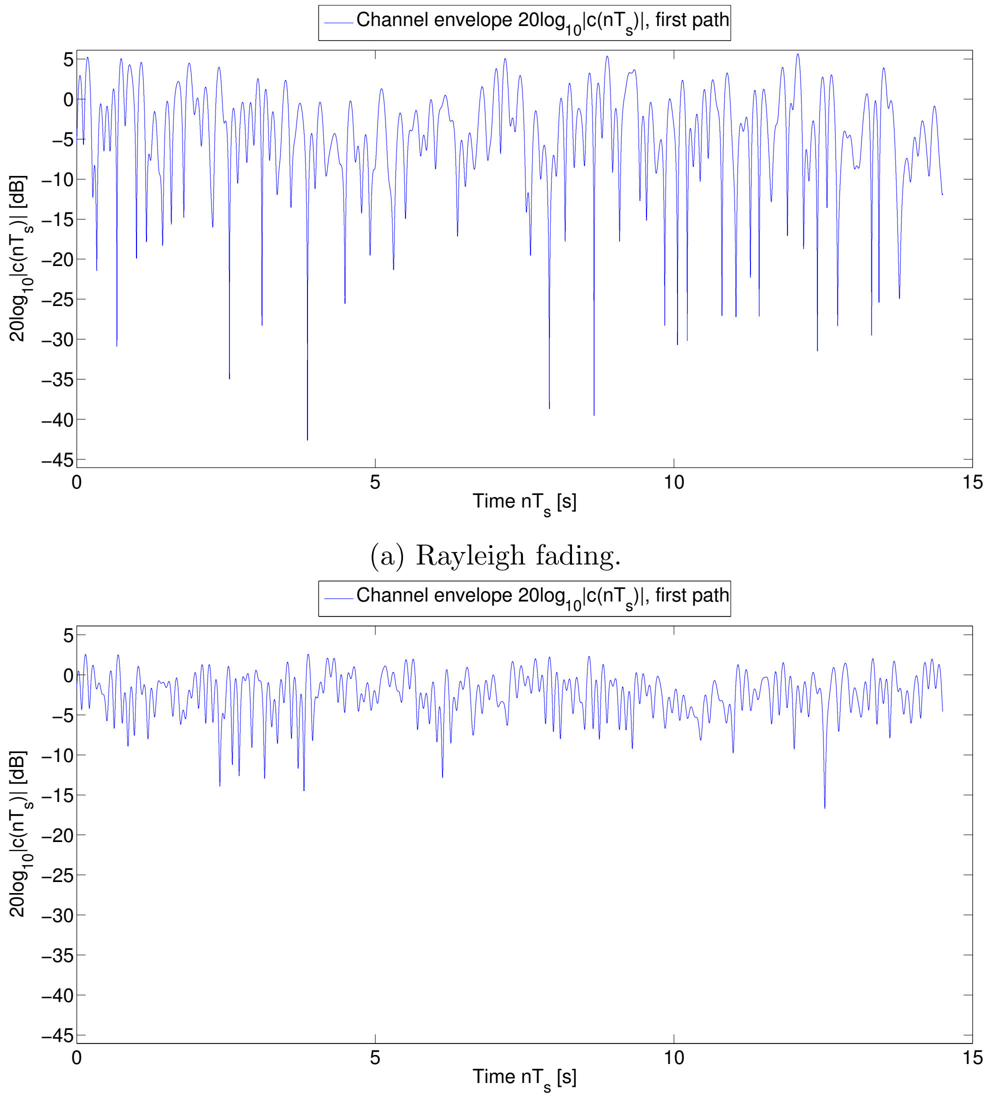

(a) Rayleigh fading.

(b) Rician fading.

Figure 13: Channel envelope for Rayleigh fading (a) and Rician fading (b).

Figure 14 shows the autocorrelation of the in-phase and quadrature-phase components of the channel coefficients of the first path of a Rayleigh fading channel simulation and the theoretical autocorrelation of these two components. The autocorrelation should be approximately the same for all Rayleigh fading paths and in Figure 14, the delay axes have been normalised relative to the maximum Doppler shift f_d. If the maximum Doppler shift is large it would require less time delay τT_s for the in-phase and quadrature-phase components to decorrelate. This means that the time at which the in-phase and quadrature-phase components decorrelate the first time is dependent on the maximum Doppler shift. However, if the axes are normalised this effect is removed and the autocorrelation for different maximum Doppler shifts can easily be compared. The expression for the theoretical autocorrelation is given by (22). Theoretically the autocorrelation should be 0 at $f_d \tau T_s = 0.4$ [5, page 74] which would then imply that the in-phase and quadrature-phase components of the channel coefficients would have zero correlation with themselves at that point for this path. The value of $f_d \tau T_s = 0.4$ is included in Figure 14 and it can be seen that the simulated in-phase and quadrature-phase components of the channel coefficients (of the first path) have an autocorrelation close to zero at that point. Since the delays τ have the unit [samples], they have to be multiplied with the time between two samples, T_s, so that the delays represent time delays and not sample delays.

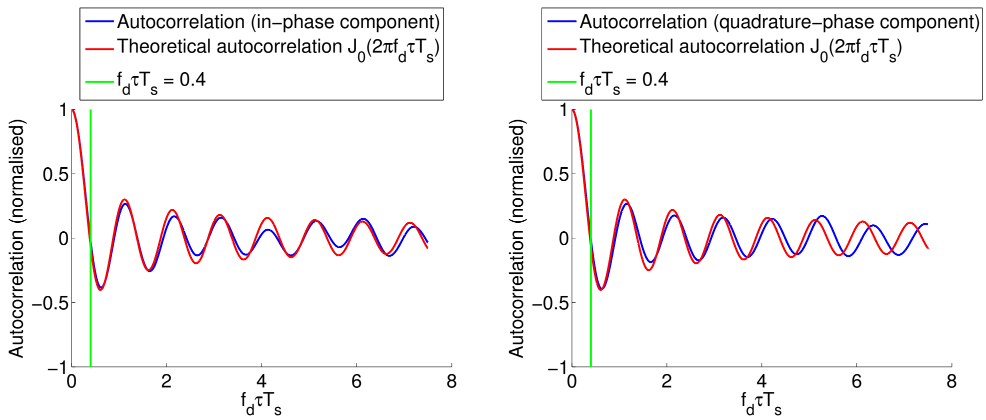

Figure 14: Autocorrelation of in-phase and quadrature-phase components of the channel coefficients of the first path and the theoretical autocorrelation of these two components.

Figure 15 shows a scaled version of the theoretical power spectral density of the in-phase and quadrature-phase components of the channel coefficients and the power spectral density of the in-phase and quadrature-phase components of the generated channel coefficients. The power spectral density of the in-phase and quadrature-phase components is only shown for the first path. According to the expression in (21) the variance of the in-phase and quadrature-phase components should be adjusted for and this is done for the theoretical curves in Figure 15. It can be seen that there is a relatively good agreement between the theoretical curves and the power spectral density of the in-phase and quadrature-phase components of the generated channel coefficients. The power spectral densities were calculated in the frequency interval $[-f_s/2, f_s/2]$ at N discrete frequencies, where N is the number of samples. In the figure, $m/(NT_s)$ are the discrete frequencies at which the power spectral densities were calculated. The sampling frequency $f_s = 1$ [MHz] was used and m represent numbers in the interval $[-N/2, N/2]$.

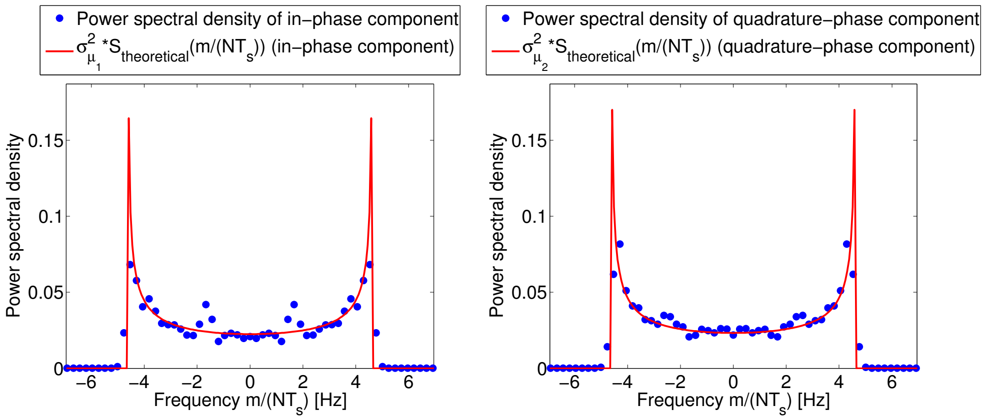

Figure 15: Power spectral density of in-phase and quadrature-phase components of the channel coefficients of the first path and a scaled version of the theoretical power spectral density of these two components.

Figure 16 shows how the amplitude of the channels varies with both time and delay for multipath fading channels, i.e. the time-varying impulse responses of the channels are shown. Both Rayleigh fading and Rician fading can be seen in the figure through Figure 16a respective Figure 16b. It can be seen that at the selected delays, the channel amplitude is non-zero and it is zero everywhere else. The actual lengths of the delay axes of both figures were 250 but since the channel amplitude is zero for delays over 8 [μs], the delay axes have been shortened. For the Rician fading channel in Figure 16b, a Rician K-factor of 5 was used. The first path has Rician fading and the second path has Rayleigh fading.

Figure 17 shows how the amplitude of the channels varies with both time and frequency for multipath fading channels, i.e. the time-varying frequency responses of the channels are shown. Both Rayleigh fading and Rician fading can be seen through Figure 17a respective Figure 17b. The frequency

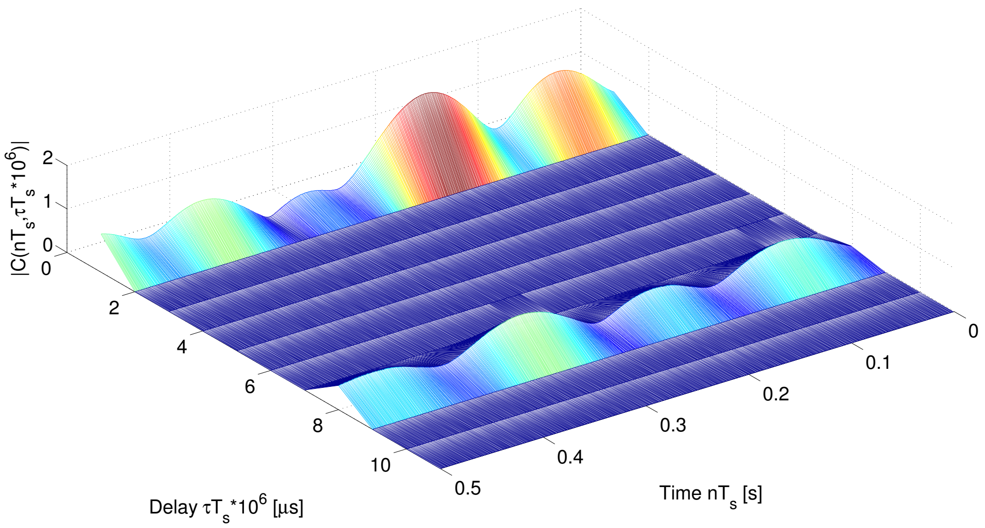

(a) Rayleigh fading.

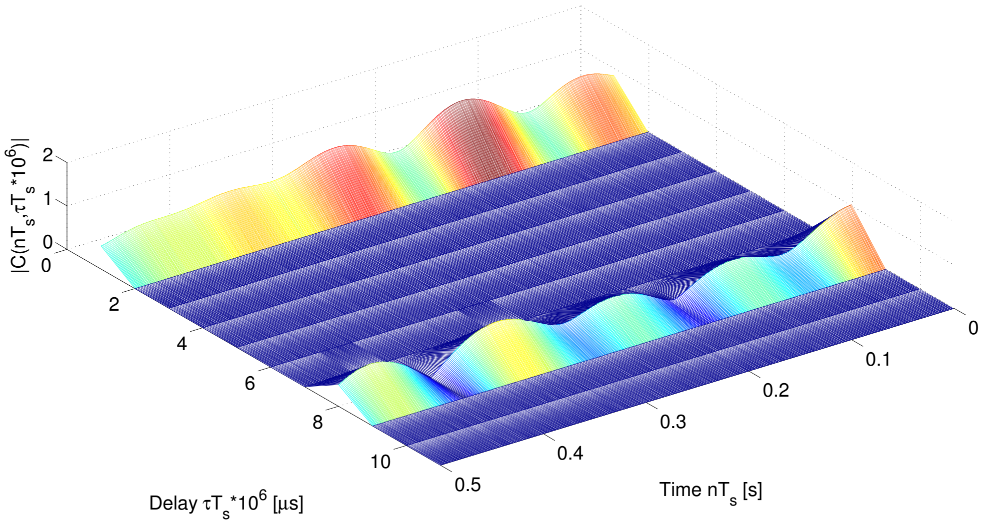

(b) Rician fading.

Figure 16: Channel amplitude as a function of time and delay for Rayleigh fading (a) and Rician fading (b).

responses that are shown in Figure 17 were given by calculating the FFT of the impulse responses in Figure 16 in the dimension along the delay axis for Rayleigh respective Rician fading. It can be seen that both channels have the frequency-selective property that was wanted to simulate meaning that the performance of the transmission varies depending on which frequency the transmission is performed at. When calculating the FFT of the channels in Figure 16, the whole impulse responses were used meaning that the delay axes reached 250 [μs] and not 11 [μs] as in the figure. The time-varying frequency responses were calculated in the frequency interval $[-f_s/2, f_s/2]$ at 250 discrete frequencies and $f_s = 1$ [MHz] was used. In the figure, $m/(MT_s)$ are the discrete frequencies at which the time-varying frequency responses were calculated. The constant M was 250 and m are numbers in the interval $[-M/2, M/2]$.

Figure 18 shows excerpts of the in-phase and quadrature-phase components of the FM signal after a Rayleigh fading channel and an excerpt of the information. The amplitude varies more in Figure 18 than in Figure 9. This is expected due to the multipath fading.

4.3 Path loss and shadowing

As was mentioned in section 2.2.2, the shadowing was implemented in terms of a filter. Figure 19 shows the autocorrelation of the noise (input to the filter), autocorrelation of the simulated shadowing (output of the filter) and the theoretical autocorrelation for the implemented shadowing model. The autocorrelation curves in Figure 19 have been normalised by division with respective autocorrelation curve's maximum value. It can be seen that the noise is uncorrelated which is expected and it can be seen that there is a difference between the autocorrelation of the simulated shadowing and the theoretical autocorrelation of shadowing. This difference has been observed when the sampling frequency is high (around 1 [MHz]) but when the sampling frequency is decreased, these two autocorrelations become very similar.

By using $|k|vT_s = X_c$ for the expression in (12), the number of samples $|k|$ required to describe the decorrelation distance X_c can be found. With a decorrelation distance of 50 [m], a velocity of 50/3.6 [m/s] and a sampling frequency of 1 [MHz], the number of samples required to describe the decorrelation distance is

$$1 \cdot 10^6 \left[\frac{\text{samples}}{\text{s}}\right] \frac{50\,[\text{m}]}{\frac{50}{3.6}\left[\frac{\text{m}}{\text{s}}\right]} = 3.6 \cdot 10^6\,[\text{samples}].$$

With a high sampling frequency one idea could be that more samples would be needed to get good performance of the autocorrelation of shadowing. When decreasing the sampling frequency but keeping the number of samples fixed, less number of samples are required for decorrelation but there would still be many samples, which would give good performance of the autocorrelation. It can be emphasised that the shadowing is random so the autocorrelation changes from simulation to simulation and sometimes the autocorrelation can have good performance also for a high sampling frequency.

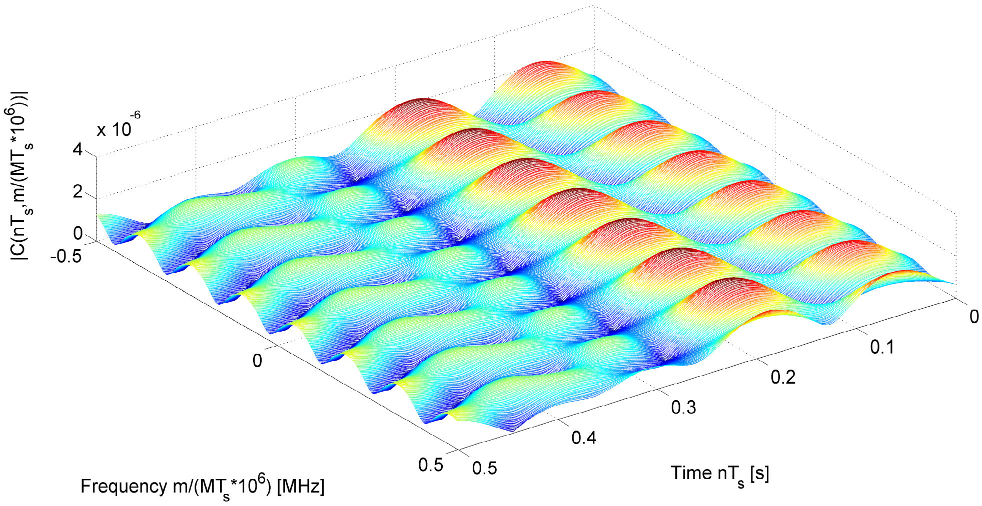

(a) Rayleigh fading.

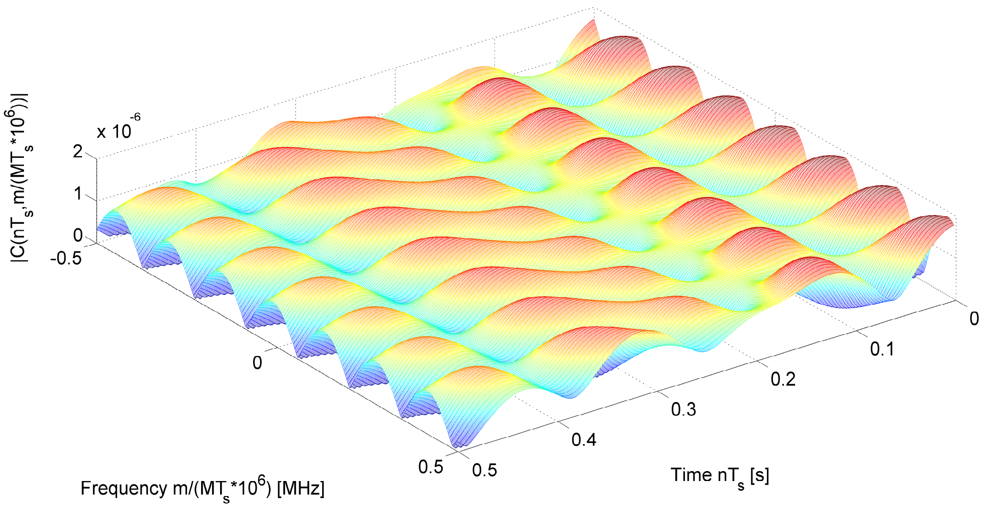

(b) Rician fading.

Figure 17: Channel amplitude as a function of time and frequency for Rayleigh fading (a) and Rician fading (b).

Figure 20 shows the noise and the simulated shadowing, i.e. the input to respective the output of the filter. It can be seen that the noise has mean zero and very little variance while the shadowing has more variance which is motivated by the fact that the shadowing samples are correlated and there are very many samples so the shadowing value can increase slowly to reach

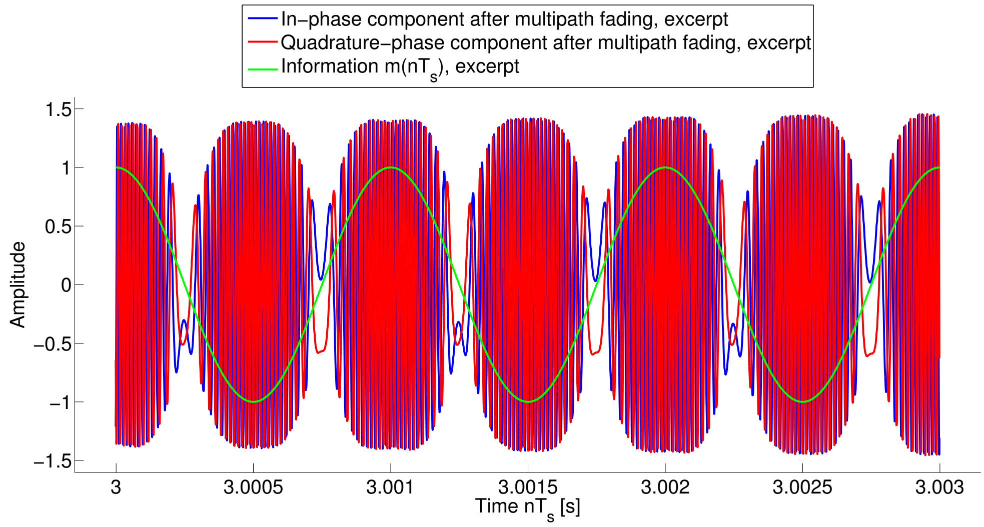

Figure 18: Excerpts of the in-phase and quadrature-phase components of the FM signal after a Rayleigh fading channel and an excerpt of the information.

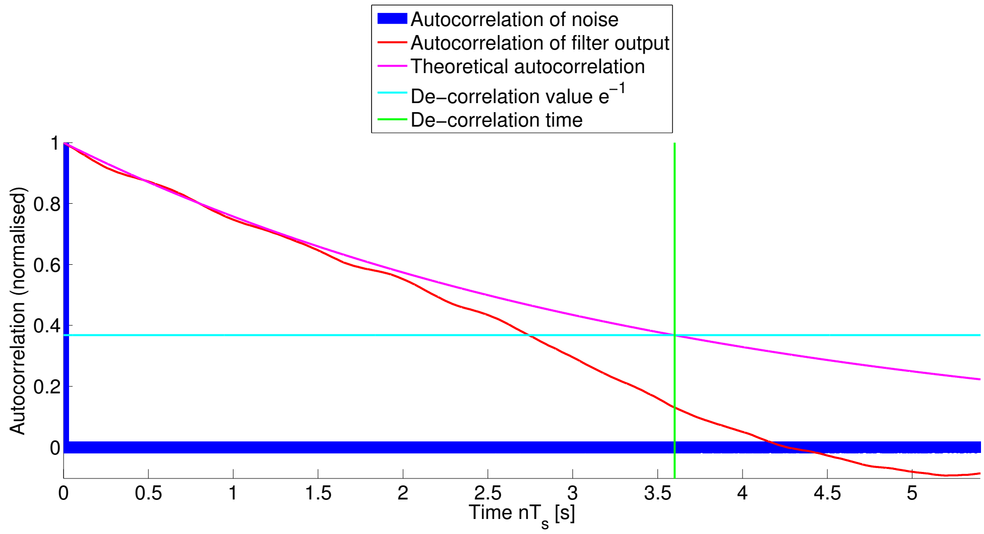

Figure 19: Autocorrelation of shadowing.

a relatively large value.

Figure 21 shows the effects of path loss, shadowing and multipath fading as a function of the logarithm of distance. The multipath fading effects only from the first path are shown in the figure. Through Figure 21a and Figure 21b, the figure contains multipath fading effects both for Rayleigh fading and Rician fading. The logarithm of the distance is used because it

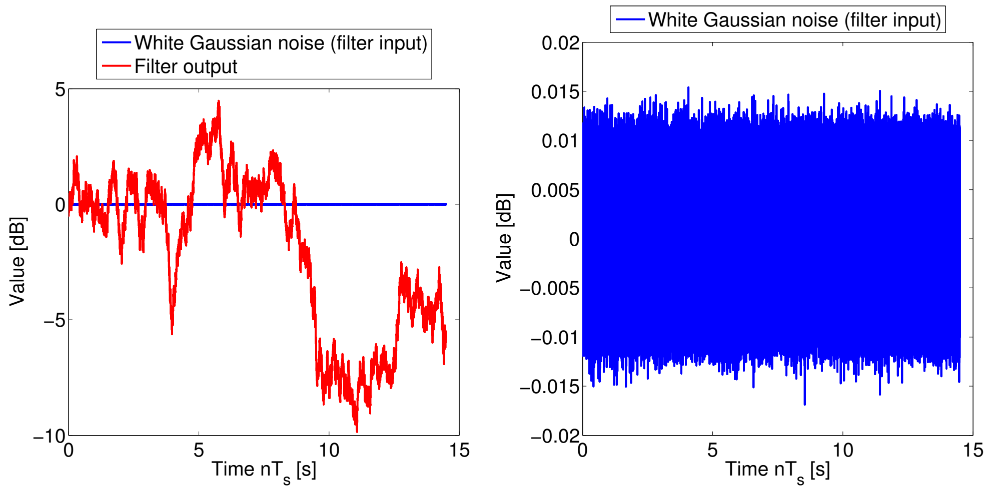

Figure 20: Noise and filter output.

will create the effect that the path loss will be linear in the figure. This linearity is easier to see for longer time sequences. The car started 5 [km] from the radio station transmitter and moved with a velocity of 50 [km/h]. The car was moving away from the transmitter. It can be seen that the shadowing varies approximately around the path loss which is expected since the shadowing theoretically has mean value zero. It can be seen that the path loss is more or less constant which is also expected because the change in distance is relatively small. It can be seen that the multipath fading varies much faster than the shadowing which is correct according to theory [5, page 27]. Figure 21b shows the effects of path loss, shadowing and multipath fading (Rician fading) as a function of the logarithm of distance. It can be seen that the variations in received power is smaller for the case of Rician fading than for the case of Rayleigh fading (Figure 21a). This is expected due to less variations for Rician fading than for Rayleigh fading as was previously motivated by the line-of-sight property for Rician fading. It can be mentioned that the implemented model for shadowing and path loss is the same for paths that have the line-of-sight property and paths that do not have it.

Figure 22 shows the in-phase and quadrature-phase components of the FM signal after multipath fading and after multipath fading, path loss and shadowing. The multipath fading in this case was Rayleigh fading.

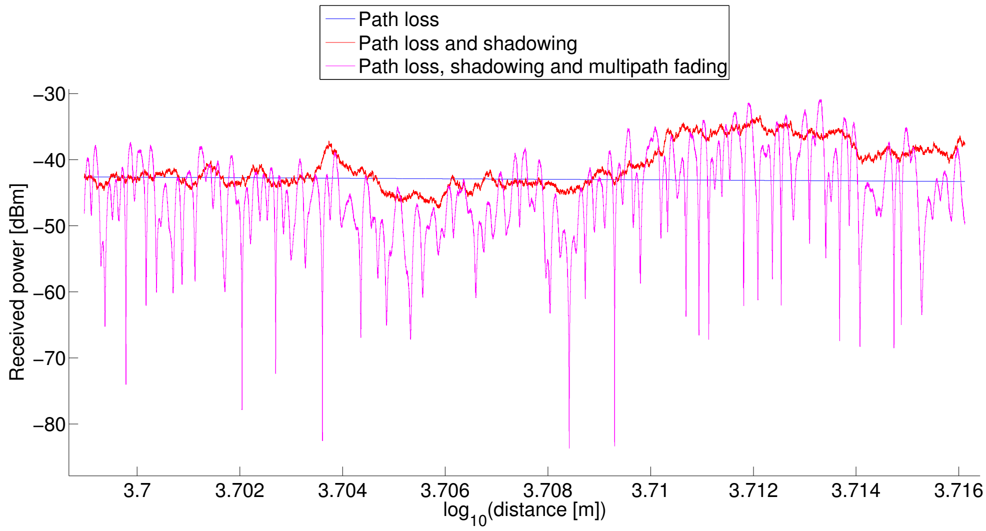

(a) Rayleigh fading.

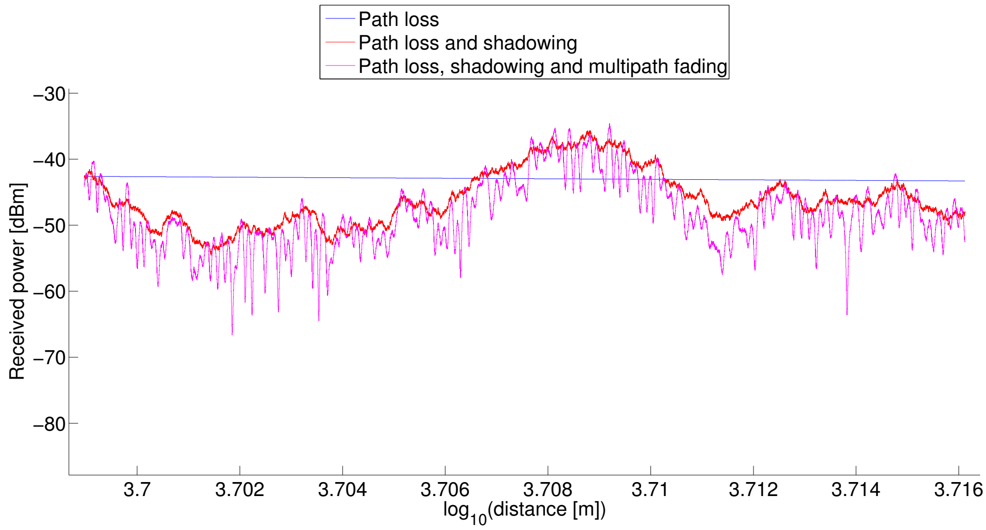

(b) Rician fading.

Figure 21: The effects of path loss, shadowing and multipath fading. In (a), the multipath fading is Rayleigh fading and in (b), the multipath fading is Rician fading.

5 Discussion

This section presents a discussion of the project. This is done by discussing the limitations of the simulator tool, possible improvements of it and suggestions on how to use it.

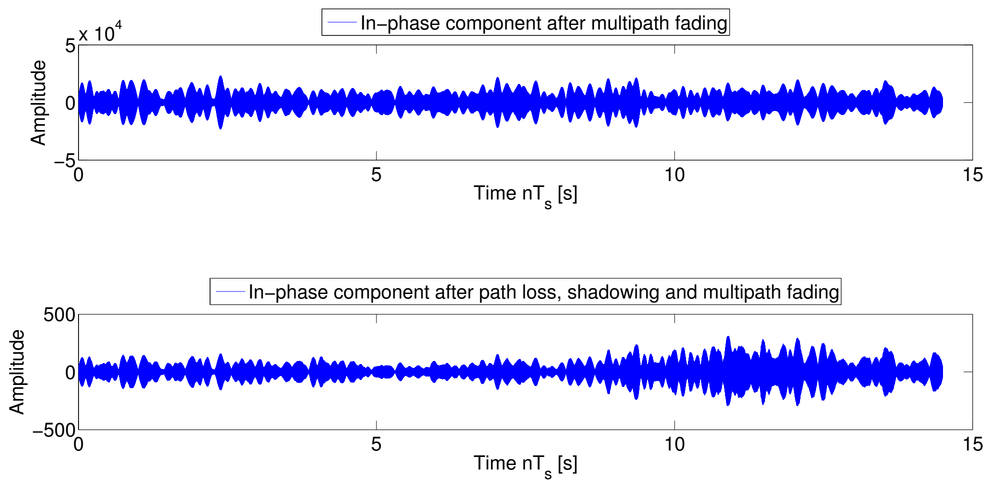

(a) In-phase component.

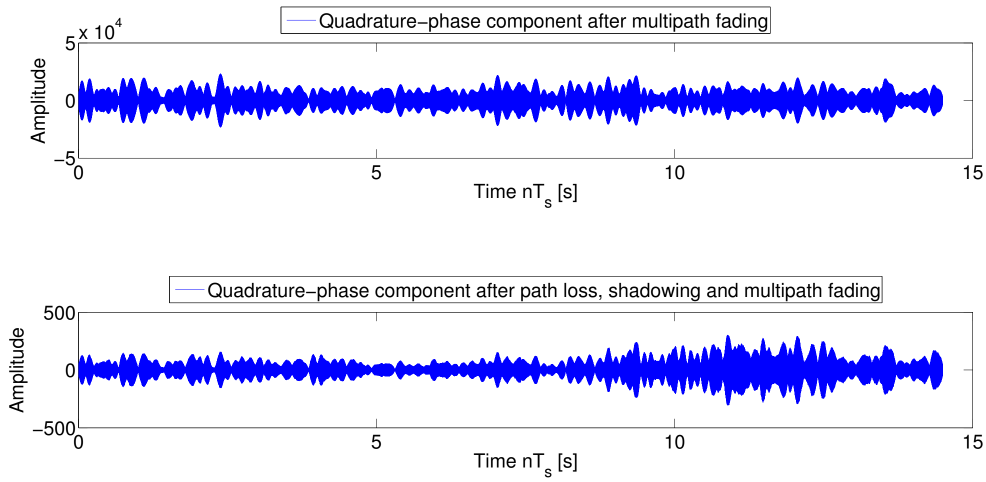

(b) Quadrature-phase component.

Figure 22: In-phase component (a) and quadrature-phase component (b) of the FM signal after multipath fading and after multipath fading, path loss and shadowing. The multipath fading is Rayleigh fading.

5.1 Limitations

The simulator tool has some limitations regarding the number of samples that can be used in the sense that it becomes somewhat slow for many samples and if the number of samples is too large, the computer's memory may not be enough. This puts a limit on how long for example the audio files can be and if the files are too long, the files will be shortened to avoid long simulation times. To have short files/signals is typically not a problem because the URT instrument has functionality for repetition. If for example a sinusoid or an audio file is used, a length of around 14.5 [s] can be enough if repetition is used. A sinusoid with a length around 14.5 [s] would be the result of the default settings. It has been noticed that if a DAB file is loaded into the simulator tool, an appropriate length of that recording is around 60 [s] and the output of the multipath fading channel then requires long time for calculation with a high sampling frequency.

In contrast to FM radio signal generation, the simulator tool does not have the possibility to create a DAB radio signal from the very beginning. The project had an emphasis on FM radio and to implement the error coding for a DAB radio COFDM system could require much additional time and is beyond the scope of this thesis. The computational time for simulations related to DAB radio has been large because of the length of the recordings in that case. Therefore the number of cases related to DAB radio that has been tested is smaller than for FM radio.

5.2 Possible improvements

The described limitation in section 5.1 about time and memory can be investigated. It can be investigated if it is possible to perform for example the calculations of the output of the multipath fading channel in a more block-oriented way meaning that the output of the multipath fading channel is calculated for a limited number of samples (a block) and the result can be written to file. Then this process is repeated for several blocks and the result of each block is written to the same file. This may remove some requirements for memory in the computer.

One functionality that could improve the possibilities for performing extensive testing with the simulator tool is to implement functionality for remote control of the URT instrument (which is possible). If the simulator tool is also modified so that a set of several simulations can be scheduled, a large number of simulations can be tested by using the URT instrument to pass the simulated output to a radio. Then this testing can for example be performed over nights. Remote control is expected to give good possibilities of testing for example multipath fading in a more automated way for several releases of radio software and with suppliers' radio proposals. It can be emphasised that for this testing to work, it has to be decided what performance measures that should be measured. For DAB radio it may be reasonable to measure the BER values.

It would be interesting to also study if it would be possible to include TV broadcasts in the simulator tool. Then the simulator tool would cover FM radio, DAB radio and TV and thereby a large part of the most used broadcasts in a car.

In the simulator tool, the user can not use delay 0 [samples] since the delay represents a number of a row of at least two matrices and in MATLAB, row 0 of a matrix is not possible to create. The smallest delay that can be used is 1 [sample] and with a sampling frequency of 1 [MHz] this represents a delay of 1 [μs]. However, the output of the multipath fading channel in the tool is being calculated with start at time 0 [s] so it means that since the delay is always at least one sample, the first output value is zero. The interpretation is that because of the non-zero delay, no signal has arrived at the receiver at time 0 [s]. Since the number of samples of the output does not take the delays into account and since the output starts at time 0 [s], the very last sample of the signal is not part of the output if the minimum delay of 1 [sample] is used. The interpretation is that because of the delay, the signal arrives too late. To not be able to use zero as the minimum delay and to miss signal/signals in the end are seen as minor issues. In fact, it is a question of how multipath fading is to be interpreted. However, it can be good to mention for full understanding of the implementation.

5.3 Suggestions on usage of simulator tool

The tool should be used to create realistic scenarios of multipath fading, path loss and shadowing. Especially it should be emphasised that many combinations of these effects can be simulated and tested. In that sense the simulator tool has an advantage compared to performing testing by using a car to drive in different environments. It may be difficult to find appropriate environments for radio testing and there may be little knowledge about the scenarios of multipath fading, path loss and shadowing. In the simulator tool, many combinations of for example number of paths and car velocity can be tested. In reality it may be difficult to know the number of paths and to adjust the velocity, the driver needs to drive in the same environment several times, with a different velocity each time.

6 Conclusion

This section presents the conclusion that can be done from the project. Especially the conclusions regarding the questions in section 1.5 are presented where each question is addressed in a separate section.

6.1 Accuracy of model

The model, which was implemented in terms of a simulator tool, has shown good agreement with theory. For the analog FM radio technique, signals can be created from scratch and thereby there are good possibilities to see the effects of multipath fading, path loss and shadowing. This is because the signal can go from being a perfect FM radio signal to having multipath fading effects introduced and finally possibly also having path loss and shadowing effects added. Since all of these effects have shown good agreement with theory on an individual basis, the model should be accurate for the analog FM radio case. Similar arguments can be mentioned for DAB radio but some precision may be lost due to the fact that a DAB radio signal can not be created from the beginning. The loaded recording may already have experienced for example path loss and shadowing effects. The fact that a DAB radio signal can not be created in the simulator tool, was a question of accuracy versus complexity. Implementing DAB radio signal generation is complex and would not have been feasible within this time-limited project.

6.2 Time and frequency dependent broadcast reception performance

Due to multipath fading, the broadcast reception performance will vary with both time and frequency. Variations in frequency are due to the signal reaching the receiver via several paths. Variations in time occur by having a velocity of the car that is greater than zero. If there is only one path in the channel, there will be no variations in frequency and if the velocity of the car is zero, there will be no variations in time. For a velocity greater than zero, the variations in time are not only due to the channel's multipath fading effects but also due to the channel's effects of path loss and shadowing. Depending on the environment, for example the decorrelation distance for shadowing can be changed to describe different sizes of objects. The velocity is relevant for all effects but perhaps least relevant for the path loss because the time sequences used in the project are relatively short. This means that the path loss does not change very much with time because the car does not move very long.

6.3 Environments

Urban environments are important to include in the model. This is because in urban environments there are many buildings and objects meaning that shadowing and multipath fading effects will occur. Path loss will occur in all environments.

6.4 Fading models

It is relevant to describe multipath fading both in the case of not having the possibility of line-of-sight communication and when there is line-of-sight communication. By doing this many cases of multipath fading are covered in the model. The Doppler spreading will imply that the multipath fading channel changes with time when the car is in motion and this holds for both Rayleigh fading and Rician fading. When the car is not in motion there can still be multipath fading but the multipath fading channel will not change with time. This case is not especially relevant for this project since a car may often be in motion. However, it may be useful to simulate also this case and it is possible to do in the simulator tool.

6.5 Same model for analog and digital techniques

It is possible to use the same model for analog and digital radio techniques. This has been seen when using DAB radio recordings in the simulator tool since the multipath fading channel works well in that case. It works well in the sense that the simulator tool can apply the multipath fading effects in the same way as for FM radio. It has been seen that the BER values have been higher when using multipath fading for DAB radio than when not using multipath fading for DAB radio. This is an expected result due to the multipath fading. The effects of path loss and shadowing should also work well with DAB radio but as was mentioned in section 6.1 some precision may be lost when using recordings. If the loaded recording is a weak signal, it may not be reasonable to add path loss and shadowing to it because the path loss may make the signal too weak. As long as the signal in the simulator tool is a baseband signal it should not matter if an analog or digital radio technique is to be used.

References

[1] The ITU Radiocommunication Assembly. RECOMMENDATION ITU-R BS.450-3 Transmission standards for FM sound broadcasting at VHF. http://www.itu.int/dms_pubrec/itu-r/rec/bs/R-REC-BS.450-3-200111-I!!PDF-E.pdf. Used at 2015-05-15.

[2] Bore-Kuen Lee, Yuan-Ho Chen, and Bor-Sen Chen. Robust H_∞ Power Control for CDMA Cellular Communication Systems. *IEEE TRANSACTIONS ON SIGNAL PROCESSING, VOL. 54, NO. 10, OCTOBER 2006*, 2006.

[3] Matthias Pätzold, Raquel Garcia, and Frank Laue. Design of High-Speed Simulation Models for Mobile Fading Channels by Using Table Look-Up Techniques. http://citeseerx.ist.psu.edu/viewdoc/download?doi=10.1.1.13.923&rep=rep1&type=pdf. Used at 2015-09-16.

[4] Cihan Tepedelenlioğlu, Ali Abdi, and Georgios B. Giannakis. The Ricean K Factor: Estimation and Performance Analysis. *IEEE TRANSACTIONS ON WIRELESS COMMUNICATIONS, VOL. 2, NO. 4, JULY 2003*, 2003.

[5] Andrea Goldsmith. *Wireless Communications*. Cambridge University Press, 2005. ISBN 978-0-521-83716-3. ELECTRONIC ISBN: 978-1-60119-764-1.

[6] Wolfgang Hoeg and Thomas Lauterbach (eds). *Digital Audio Broadcasting-Principles and Applications of DAB, DAB+ and DMB, Third Edition*. John Wiley & Sons © 2009, 2009. ISBN 9780470510377.

[7] NATIONAL INSTRUMENTS. What is I/Q Data? http://www.ni.com/tutorial/4805/en/. Used at 2015-05-03.

[8] Ph.D. Lawrence Der. Frequency Modulation (FM) Tutorial. http://www.silabs.com/Marcom%20Documents/Resources/FMTutorial.pdf. Silicon Laboratories Inc. Used at 2015-05-29.

[9] Cyril-Daniel Iskander (Hi-Tek Multisystems). A MATLAB®-based Object-Oriented Approach to Multipath Fading Channel Simulation. http://www.mathworks.com/matlabcentral/fx_files/18869/1/ChannelModelingWhitePaper.pdf. Used at 2015-09-13.

[10] Ken Schwaber and Jeff Sutherland. The Scrum Guide™. http://www.scrumguides.org/docs/scrumguide/v1/Scrum-Guide-US.pdf#zoom=100, July 2013. Used at 2015-05-31.

[11] J.H. Stott. The how and why of COFDM. http://downloads.bbc.co.uk/rd/pubs/papers/pdffiles/ptrev_278-stott.pdf. BBC Research and Development. Used at 2015-05-31.

[12] The MathWorks, Inc. Fading Channels. http://se.mathworks.com/help/comm/ug/fading-channels.html, . Used at 2015-05-31.

[13] The MathWorks, Inc. fitdist. http://se.mathworks.com/help/stats/fitdist.html#btu54gt-3, . Used at 2015-05-02.

[14] The MathWorks, Inc. Using RicianDistribution Objects. http://se.mathworks.com/help/stats/riciandistribution-object.html, . Used at 2015-05-02.

[15] The MathWorks, Inc. Rician Distribution. http://se.mathworks.com/help/stats/rician-distribution.html, . Used at 2015-09-16.

[16] The MathWorks, Inc. audioread. http://se.mathworks.com/help/matlab/ref/audioread.html, . Used at 2015-05-31.

[17] The MathWorks, Inc. filter. http://se.mathworks.com/help/matlab/ref/filter.html, . Used at 2015-05-22.

[18] The mathWorks, Inc. int16. http://se.mathworks.com/help/matlab/ref/int16.html. Used at 2015-05-23.

[19] The MathWorks, Inc. resample. http://se.mathworks.com/help/signal/ref/resample.html. Used at 2015-05-03.

[20] Eric W. Weisstein. "Complex Modulus." From MathWorld--A Wolfram Web Resource. http://mathworld.wolfram.com/ComplexModulus.html, . Used at 2015-09-12.

[21] Eric W. Weisstein. "Euler Formula." From MathWorld--A Wolfram Web Resource. http://mathworld.wolfram.com/EulerFormula.html, . Used at 2015-04-21.

[22] Eric W. Weisstein. "Kronecker Delta." From MathWorld--A Wolfram Web Resource. http://mathworld.wolfram.com/KroneckerDelta.html, . Used at 2015-05-05.

[23] Eric W. Weisstein. "L^2-Norm." From MathWorld--A Wolfram Web Resource. http://mathworld.wolfram.com/L2-Norm.html, . Used at 2015-09-12.

[24] Eric W. Weisstein. "Normal Distribution." From MathWorld--A Wolfram Web Resource. http://mathworld.wolfram.com/NormalDistribution.html, . Used at 2015-05-31.

A Appendix

This section is an appendix.

A.1 Header information for URT file

After the header information described in section 3.2.1, the header (which is a vector) should contain 430 elements of the number “97”. It is important to write the header information and the signal values to the .bin file in a correct way. This is done according to the following formats:

- 0 (preamble): `uint64`
- Version (1): `uint16`
- The rest of the header except for the 430 elements of the number “97”: `double`
- The number “97”: `uint8`
- The signal values: `int16`

A.2 Excel document with used settings

At next page, an Excel document with the used settings for a simulation with Rayleigh fading is included (as a .pdf file). The name of the file is “UsedSettings_21_Jun_2015_21_33_14.xls” where the date and time in the name is when the document was created.

Carrier frequency [MHz]	100
Message frequency [Hz]	1000
Sampling frequency [MHz]	1
Signal length [samples]	14500000
Signal amplitude	1
Frequency deviation [Hz]	75000
Number of paths	2
Velocity [km/h]	50
Number of sinusoids	70
Delay vector [samples]	1 8
Number of samples	14500000
Scaling of channel coefficients	1 0.5
Fading	RayleighFading
Rician K-factor	5
Name of folder for generated file	C:\Users\FLUNDIN
Transmit power (radio station) [kW]	60
Start distance from radio station (transmitter) [km]	5
Decorrelation distance [m]	50
Standard deviation shadowing [dB]	4
Reference distance [m]	100
Path-loss exponent (gamma)	4
Signal that was used	GeneratedFmSignal
Usage of path loss and shadowing	TRUE
Usage of sinusoid as information	TRUE
Name of generated file	GeneratedURTFile.bin